

# ObjectSeeker: Certifiably Robust Object Detection against Patch Hiding Attacks via Patch-agnostic Masking

Chong Xiang  
Princeton University

Alexander Valtchanov  
Princeton University

Saeed Mahloujifar  
Princeton University

Prateek Mittal  
Princeton University

## Abstract

Object detectors, which are widely deployed in security-critical systems such as autonomous vehicles, have been found vulnerable to physical-world *patch hiding attacks*. The attacker can use a single physically-realizable adversarial patch to make the object detector miss the detection of victim objects and completely undermines the functionality of object detection applications. In this paper, we propose ObjectSeeker as a defense framework for building certifiably robust object detectors against patch hiding attacks. The core operation of ObjectSeeker is *patch-agnostic masking*: we aim to mask out the entire adversarial patch *without any prior knowledge* of the shape, size, and location of the patch. This masking operation neutralizes the adversarial effect and allows any vanilla object detector to safely detect objects on the masked images. Remarkably, we develop a certification procedure to determine if ObjectSeeker can detect certain objects with *a provable guarantee against any adaptive attacker within the threat model*. Our evaluation with two object detectors and three datasets demonstrates a significant ( $\sim 10\%$ - $40\%$  absolute and  $\sim 2$ - $6\times$  relative) improvement in certified robustness over the prior work, as well as high clean performance ( $\sim 1\%$  performance drop compared with vanilla undefended models).

## 1 Introduction

Object detectors, which aim to output a list of bounding boxes detecting every object in a given image, have been shown vulnerable to *patch hiding attacks* [23, 58, 60, 65, 71, 76]. The patch hiding attack aims to make object detectors miss the detection of victim objects (e.g., making an autonomous vehicle miss a pedestrian) using an adversarial *patch* [5]. This attack can be realized in the physical world by attaching the adversarial patch to the real-world scene and thus imposes a notable threat to object detection applications like autonomous driving, augmented reality, and face recognition.

To counter the threat of patch hiding attacks, the research community has been actively seeking defense strategies. How-

ever, most existing defenses [10, 24, 28, 40, 54] are based on heuristics and lack formal security guarantees. As a result, these defenses could be broken when an attacker has full access to the defense algorithm and setup [1, 6, 7, 61]. Observing the limitations of heuristic-based defenses, Xiang et al. [68] designed DetectorGuard as the first (and the only) certifiably robust defense against patch hiding attacks. The defense aims to achieve a provable guarantee that the object detector can always make correct predictions for certain objects against any adaptive attacker within the threat model. Such certifiable robustness provides a pathway towards ending the arms race between attackers and defenders.

Despite its contributions of being the first certifiably robust defense against patch hiding attacks, DetectorGuard [68] relies on certifiably robust image *classifiers* (against adversarial patches) for achieving certifiable robustness. This dependency forces DetectorGuard to inherit (and usually amplify) the imperfection of robust image classifiers.<sup>1</sup> As a result, DetectorGuard only achieves limited robustness performance: it can only certify the robustness for  $\sim 30\%$  objects from the VOC [15] dataset and  $\sim 10\%$  of COCO [30] objects even when the attacker is restricted to placing a single patch *far away* from the victim objects. In this paper, we aim to explore a new direction for *certifiably* robust object detection: we propose ObjectSeeker, a defense that is solely based on vanilla undefended object detectors and is thus free from any flaws of robust image classifiers.

**ObjectSeeker overview.** The core idea of ObjectSeeker is to apply pixel masks to the input image and perform vanilla object detection on the masked images. If the adversarial patch is masked, the attacker has no malicious influence over the model, and any vanilla object detector can make accurate predictions. We focus on the setting that the patch hiding attacker can use one adversarial patch whose shape, size, and

<sup>1</sup>We note that more advanced certifiably robust image classifiers against adversarial patches have been proposed since DetectorGuard was published [55, 67]. However, these new robust image classifiers are too computationally expensive to be used in the costly sliding window operation of DetectorGuard.

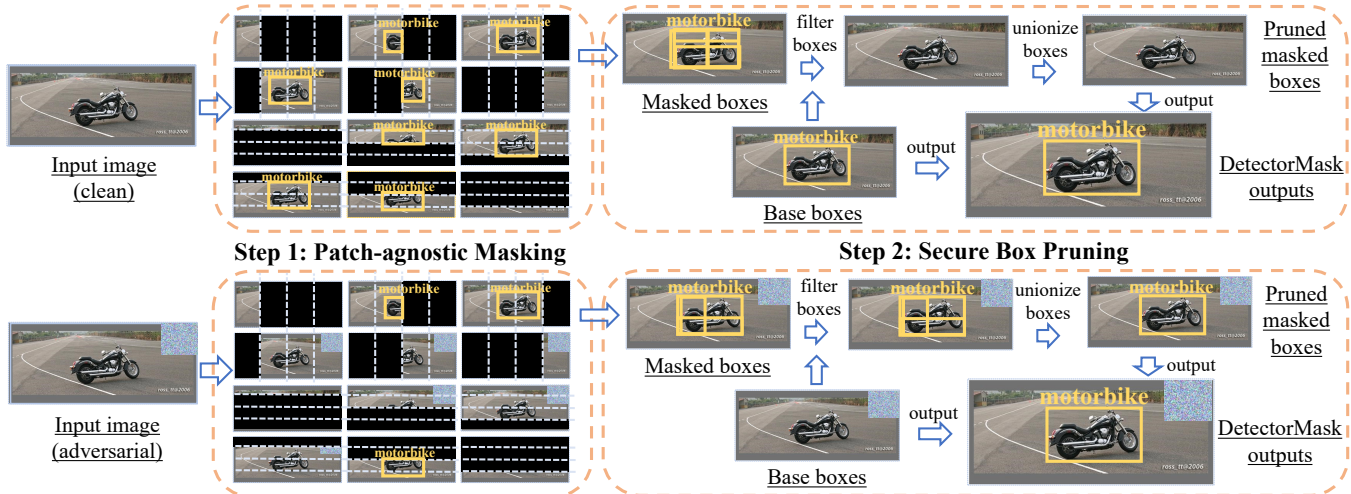


Figure 1: **ObjectSeeker Overview.** *Step 1: patch-agnostic masking.* We mask out image halves divided by a set of vertical and horizontal lines, and perform vanilla object detection on the remaining halves. This masking operation is agnostic to patch shape, size, and location. *Step 2: secure box pruning.* We use a “robust” similarity score to identify and *filter* redundant masked boxes (predicted on the masked images) that are duplicates of the base boxes (predicted on the original images); we then *unionize* the remaining masked boxes. Finally, we combine pruned masked boxes and base boxes as the defense output. In the *clean* setting (top of the figure), the motorbike is detected by both base and masked boxes. All masked boxes are pruned, and we finally output the base box. In the *adversarial* setting (bottom of the figure), the motorbike is only detected by masked boxes; we robustly output the unionized masked boxes.

location are unknown to the defender; we aim to solve two major research questions: (1) How can we generate masks that can remove the patch without knowing the patch location, shape, and size? (2) How can we achieve certifiable robustness while maintaining high clean performance? Our ObjectSeeker solution involves two steps of *patch-agnostic masking* and *secure box pruning*; we provide a defense overview in Figure 1.

*Step 1: patch-agnostic masking.* The first step of ObjectSeeker is to generate and apply pixel masks (left of Figure 1). We aim to generate a set of masks such that some of the masks can remove the entire adversarial patch regardless of the shape, size, and location of the patch. Towards this end, we propose to mask out *image halves*: we divide the image into halves using a set of vertical and horizontal lines, mask out each image half, and perform object detection on the other half. Intuitively, for a patch of any shape, size, and location, we can find a set of lines that do not intersect with the patch to generate image halves that can mask out the entire patch. As long as the patch is reasonably sized and does not corrupt the entire victim object, a vanilla object detector is likely to detect the object from the remaining benign pixels. In Section 3.1, we can further demonstrate that our masking strategy allows the object detector to safely see most of the image pixels without any interference from the adversary. This lays a foundation for robust object detection.

*Step 2: secure box pruning.* Despite its robustness property, the pixel masking operation can introduce duplicate boxes and downgrade the precision of the model prediction; this is

because an object can be detected multiple times on different masked images (see Figure 1 for visual examples). The second step of ObjectSeeker aims to remove these redundant boxes for precise prediction outputs while preserving the robustness property achieved by the masking operation. Towards this goal, we use a “robust” box similarity score to identify similar boxes and prune redundant boxes accordingly. This process is illustrated in the right of Figure 1 and will be discussed in Section 3.2.

*Certifiable robustness.* Remarkably, our ObjectSeeker design allows us to develop a certification procedure to certify if ObjectSeeker has a provable robustness guarantee for a given object. In Section 3.3, we prove that if a vanilla object detector predicts a “good” bounding box for a given object in a masked image without any adversarial pixels, ObjectSeeker can always detect the object no matter what an adaptive patch hiding attacker within the threat model does.

**State-of-the-art certified robustness across benchmark datasets.** We implement ObjectSeeker with two vanilla object detectors: YOLOR [62] and Mask R-CNN [22] with a Swin Transformer backbone [35], and evaluate it on three object detection datasets: VOC [15], COCO [30], and KITTI [17]. We demonstrate that ObjectSeeker achieves significant ( $\sim 10\%$ - $40\%$  absolute and  $\sim 2\text{-}6\times$  relative) improvements in certified robustness over DetectorGuard [68]. In the meantime, ObjectSeeker also has similarly high clean performance as vanilla undefended models ( $\sim 1\%$  clean performance drops). Our contributions can be summarized as follows.

- We propose ObjectSeeker as a certifiably robust defense framework for any vanilla object detector via a patch-agnostic masking strategy.
- We develop a certification procedure to determine if ObjectSeeker is provably robust for certain objects against any patch hiding attack within the threat model.
- We implement and evaluate ObjectSeeker on object detection benchmark datasets and demonstrate significant robustness improvements over DetectorGuard [68].

## 2 Background and Problem Formulation

In this section, we introduce the task of object detection, attack formulation, and defense formulation.

### 2.1 Object Detection

The task of object detection is to predict a list of bounding boxes that locate and classify each object in a given image. We use  $\mathbf{x} \in \mathcal{X} \subset [0, 1]^{W \times H \times 3}$  to denote the input image with width  $W$ , height  $H$ , and 3 color channels (image pixels are re-scaled to  $[0, 1]$ ). We use  $\mathbf{b} = (x_{\min}, y_{\min}, x_{\max}, y_{\max}, \ell, c)$  to represent a bounding box, where four coordinates  $(x_{\min}, y_{\min}, x_{\max}, y_{\max})$  illustrate the box,  $\ell$  denotes the class label, and  $c \in [0, 1]$  denotes the prediction confidence for this box detection. An object detector takes an image  $\mathbf{x}$  as the input and outputs a list of boxes  $\mathbf{b}_0, \mathbf{b}_1, \dots, \mathbf{b}_n$ . We further use an unordered set  $\mathcal{B} = \{\mathbf{b}_0, \mathbf{b}_1, \dots, \mathbf{b}_n\}$  to denote the detection output and let  $\mathcal{O}$  denote the space of all possible  $\mathcal{B}$  (detection outputs). We can then formally represent an object detector as  $\mathbb{F}(\mathbf{x}) : \mathcal{X} \rightarrow \mathcal{O}$ . We sometimes abuse the notation by using  $\mathbb{F}(\mathbf{x}, \gamma) : \mathcal{X} \times [0, 1] \rightarrow \mathcal{O}$  to denote object detection that only considers boxes with confidence higher than  $\gamma$ . We do not make any assumption on the object detector  $\mathbb{F}$ , it can be any off-the-shelf model such as YOLO [4, 50, 62], Faster R-CNN [53], and Mask R-CNN [22].

**Box operation.** There are several important box operations. We use  $|\mathbf{b}|$  to denote the *area* of the box  $\mathbf{b}$ . We use  $\mathbf{b}_0 \cap \mathbf{b}_1$  and  $\mathbf{b}_0 \cup \mathbf{b}_1$  to denote the *intersection* and *union* of two boxes, respectively. When two boxes have different class labels, their intersection is *empty* and their union is undefined.

**Performance evaluation.** To evaluate a conventional object detector, we consider a detected box is correct if (1) the box class label matches the ground-truth box label, (2) and Intersection over Union (IoU) between the detected box and the ground-truth box, defined as  $|\mathbf{b}_0 \cap \mathbf{b}_1| / |\mathbf{b}_0 \cup \mathbf{b}_1|$ , exceeds a certain threshold. We count a correct detected box as a true-positive (TP). On the other hand, any detected box that is not a TP is a false-positive (FP); any ground-truth box that is not correctly detected is a false-negative (FN). Furthermore, we define *precision* as  $TP / (TP + FP)$  and *recall* as  $TP / (TP + FN)$ . We aim to build object detectors that have both high precision and high recall.

### 2.2 Attack Formulation

We focus on defending against patch hiding attacks.

**Objective: hiding attacks.** The hiding attack aims to make the object detector miss the detection of the victim object, which increases FN errors and downgrades the detection recall. This attack can cause serious consequences in real-world scenarios such as an autonomous car failing to detect and consequently hitting a pedestrian.

**Means: patch attacks.** The patch attack aims to generate adversarial pixels within a local region (forming a patch) to cause mispredictions of the machine learning model. This attack can be realized in the physical world by printing and attaching the patch to the underlying scene and thus imposes an urgent threat to real-world machine learning applications. Formally, we denote the patch region with a binary tensor  $\mathbf{p} \in \{0, 1\}^{W \times H}$  of the same shape as the  $W \times H$  input image  $\mathbf{x}$ . We set the elements within the patch region to zeros, and the rest to ones. We further use  $\mathcal{P}$  to denote a set of patch regions  $\mathbf{p}$  that an attacker can use. Then, the constraint set of the patch attack can be represented as  $\mathcal{A}_{\mathcal{P}}(\mathbf{x}) = \{\mathbf{x} \odot \mathbf{p} + \mathbf{x}' \odot (\mathbf{1} - \mathbf{p}) \mid \mathbf{x} \in \mathcal{X}, \mathbf{p} \in \mathcal{P}\}$ . Here,  $\mathbf{x}' \in [0, 1]^{W \times H \times 3}$  is the content of the patch and is under the *arbitrary* control of the attacker.

We note that the patch region  $\mathbf{p}$  is determined by the number of patches, patch shape, patch size, and patch location. In this paper, we focus on the setting that the attacker can use *one patch whose shape, size and location are unknown to the defender*. The defending role in this setting is a challenging research question because the attacker can arbitrarily control the content, shape, size, location of the patch.<sup>2</sup>

**Remark.** We follow DetectorGuard [68] and focus on the patch hiding attack. The hiding attack is a fundamental attack against object detectors since it completely disrupts the function of detecting objects. The patch attack is a common physically-realizable attack and thus imposes a notable threat to object detectors, most of which interact intensely with the physical world. Therefore, defending against patch hiding attacks is important for the safe deployment of object detectors.

### 2.3 Defense Formulation

In this section, we formulate the defense problem.

**Defender knowledge.** As discussed in Section 2.2, we consider patch hiding attacks that use one patch of any content, shape, size, and location. The defender only knows that there might be one adversarial patch on the input image, but does not know any other information about the patch. The defender can use any off-the-shelf undefended object detector to build the defense model.

**Robustness definition.** Facing a patch hiding attack, our defense aims to robustly predict bounding boxes that *cover*

<sup>2</sup>We note that the defense problem can become meaningless when the patch occludes the entire object; in this case, no one (not even a human) can detect the completely invisible object.

Table 1: Summary of important notation

Notation	Description	Notation	Description
$\mathbf{x} \in \mathcal{X}$	input image	$\mathbf{b} \in \mathcal{B} \in \mathcal{O}$	bounding box
$\mathbf{m} \in \mathcal{M}$	pixel mask	$\mathbf{p} \in \mathcal{P}$	patch region
$\mathbb{F} : \mathcal{X} \rightarrow \mathcal{B}$	undefended model	$\gamma \in [0, 1]$	confidence thres.
$\mathbb{S} : \mathcal{B} \times \mathcal{B} \rightarrow \mathbb{R}$	similarity score	$\tau \in [0, 1]$	filtering thres.
$k \in \mathbb{Z}^+$	# lines	$T \in [0, 1]$	certification thres.

at least part of each object and have correct class labels. To formally discuss the robustness objective, we introduce the following concept of Intersection over Area (IoA)

**Definition 1** (Intersection over Area (IoA)). *The IoA between two boxes  $\mathbf{b}_0$  and  $\mathbf{b}_1$  is the ratio of the intersecting area of two regions to the area of the first box  $\mathbf{b}_0$ . Formally, we have:  $\text{IoA}(\mathbf{b}_0, \mathbf{b}_1) = |\mathbf{b}_0 \cap \mathbf{b}_1| / |\mathbf{b}_0|$ .*

We note that when two boxes have different class labels, we consider the intersection  $\mathbf{b}_0 \cap \mathbf{b}_1$  empty and the IoA is 0.

With the concept of IoA, we can then reiterate the robustness definition as: given a ground-truth box  $\mathbf{b}_{\text{gt}}$ , we aim to detect a box  $\mathbf{b}'$  such that  $\text{IoA}(\mathbf{b}_{\text{gt}}, \mathbf{b}') > T$ , where  $T \in [0, 1]$  determines the strength of robustness. We term this as *IoA robustness*. We choose this robustness objective because it aligns with our goal of mitigating hiding attacks; this objective is also similar to that of DetectorGuard [68] and enables a fair comparison. In Appendix B and C, we provide further discussions on other possible robustness definitions.

**Certifiable robustness.** More importantly, we target *certifiable robustness*: we aim to provide a provable guarantee that, for certain objects whose robustness can be certified by our certification procedure, no attacker within the threat model can bypass the defense (i.e., hide the objects). We will prove that our robustness certification holds for all possible attack strategies, including an adaptive attacker with perfect knowledge of our defense setup. To evaluate our defense, we will apply our certification procedure to datasets with annotated bounding boxes (objects): we term the fraction of certified objects among all annotated objects as *certified recall* and use it as our robustness metric. The reported certified recall reflects our estimation of the defense robustness when it is deployed in the wild.

### 3 ObjectSeeker Design

**Overview.** In this section, we introduce the design of ObjectSeeker, a defense framework for building certifiably robust object detectors against patch hiding attacks. ObjectSeeker operates in a two-step manner (recall the defense overview in Figure 1). First, ObjectSeeker applies a set of patch-agnostic pixel masks to the input images and performs vanilla object detection on masked images (Section 3.1). Our masking strategy ensures that some of the masks remove the entire adversarial patch so that a vanilla object detector can detect victim

objects from the unmasked regions of these images. Second, ObjectSeeker performs secure box pruning to remove redundant bounding boxes detected on different masked images (Section 3.2). This operation aims to improve the detection precision while preserving the robustness property achieved by the masking operation. Notably, with a careful design of pixel masking and box pruning, we can develop a certification procedure to determine if ObjectSeeker has provable robustness guarantees for certain objects against any adaptive attacker within our threat model (Section 3.3).

We provide the pseudocode of ObjectSeeker in Algorithm 1 and a summary of important notation in Table 1. We will discuss the details of each defense module next.

#### 3.1 Patch-agnostic Masking

In this subsection, we discuss the first step of ObjectSeeker: patch-agnostic masking.

**Intuition and challenge.** The objective of our pixel-masking defense is to mask out the adversarial patch (but not the entire victim objects) from the input image. Typically, any vanilla object detector can safely detect objects from the masked image once all adversarial pixels are removed.<sup>3</sup>

One challenge of the pixel-masking defense is ensuring that some masks can remove the entire patch without knowing how attackers generate the patch. A naive solution to this challenge, which is adopted by a few certifiably robust image classification techniques [38, 67], is to move a mask across all possible image locations and evaluate model predictions on every masked image. If the mask is large enough to cover the entire patch, at least one masked image (regardless of the patch location) has no adversarial pixels and enables safe model predictions. However, this naive approach requires additional prior knowledge of the patch shape and size to properly determine the mask shape and size. When this prior knowledge is unavailable or imprecise, the mask might fail to remove the entire patch, which completely undermines the certifiable robustness. In ObjectSeeker, we propose a patch-agnostic masking strategy to overcome this weakness.

**Masking strategy.** The robustness requirement of our patch-agnostic masking is that: for each object, we have at least one mask that removes the entire patch while preserving most of the object pixels (so that we can safely detect each object).<sup>4</sup> Towards this goal, we propose to mask out “*image halves*” determined by a set of horizontal and vertical lines; we provide visualization for this strategy in Figure 2. First, we select a set of evenly spaced horizontal and vertical lines across the image (left of Figure 2). Second, observing that

<sup>3</sup>We note that vanilla object detectors are already trained to handle partial occlusions, given that occlusions occur frequently in vanilla object detection tasks such as VOC [15] and COCO [30]. Therefore, as long as the mask removes the patch while preserving at least part of the victim object, a vanilla object detector is likely to make a correct detection.

<sup>4</sup>We note that we can use a different mask for a different object to achieve this goal (i.e., detecting different objects from different masked images).

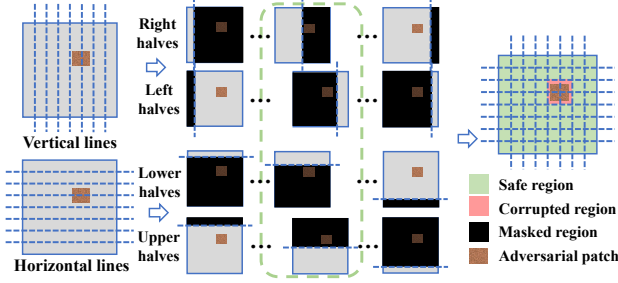


Figure 2: Visualization for pixel masking

each horizontal/vertical line splits the image into two halves, we mask out one half and perform vanilla object detection on the other half (center of Figure 2).<sup>5</sup> Remarkably, our masking strategy has two important properties.

**Property 1: agnostic to patch shape/size/location.** First, our mask set generation only requires the number of horizontal and vertical lines as its input and thus does not need any prior knowledge of the patch. For a patch of any shape, size, and location, vertical/horizontal lines that *do not intersect with the patch* can generate masks that remove the entire patch. This patch-agnostic property is a huge improvement from all existing masking-based certifiably robust defenses (for image classification) against adversarial patches [38, 66, 67, 69], whose robustness is completely undermined without a good prior estimation of the patch information.

**Property 2: preserving benign image regions.** Second, our masking strategy allows us to see most of the benign objects/pixels within image halves containing no adversarial pixels. To better understand this property, in the green dashed box of Figure 2, we visualize the smallest masks that remove the entire patch from four different directions (right, left, lower, and upper), which are given by four different lines that are closest to (but do not intersect with) the patch. From these four masked images, the object detector can see different benign halves of the image without any interference from the attacker. We further plot the union of these benign image halves as the green “safe” region on the right of Figure 2: any pixel/object in the green region can be observed from at least one masked image with no adversarial patch. We also plot the rest of the pixels as the red “corrupted” region, and it is only a small restricted region around the adversarial patch. This property allows us to preserve most of the victim objects.

**Masking pseudocode.** Now, we discuss the implementation details of the patch-agnostic masking. We present the pseudocode in Line 2-7 of Algorithm 1. The first step of pixel masking is to generate a mask set (Line 2). Formally, we represent each mask as a binary tensor  $\mathbf{m} \in \mathcal{M} \subset \{0, 1\}^{W \times H}$  that has the same shape as the  $W \times H$  images. We set the elements within the mask to 0, and others to 1.

<sup>5</sup>Our masking strategy is also compatible with other types of lines (e.g., diagonal or curved lines). We focus on vertical/horizontal lines because vanilla object detectors predict boxes bounded by vertical/horizontal lines.

---

### Algorithm 1 ObjectSeeker inference algorithm

---

**Input:** Image  $\mathbf{x}$ , image size  $(W, H)$ , base object detector  $\mathbb{F}$ , the number lines  $k$  (for masking), masked boxes confidence threshold  $\gamma_m$ , base boxed confidence threshold  $\gamma_b$ , similarity score function  $\mathbb{S}$ , box filtering threshold  $\tau$

**Output:** Robust detection results  $\mathcal{B}_{\text{robust}}$

```

1: procedure OBJECTSEEKER( $\mathbf{x}, \mathbb{F}, k, W, H, \gamma_m, \gamma_b, \mathbb{S}, \tau$ )
2:    $\mathcal{M} \leftarrow \text{MASKSET}(k, W, H)$ 
3:    $\mathcal{B}_{\text{mask}} \leftarrow \emptyset$ 
4:   for  $\mathbf{m} \in \mathcal{M}$  do
5:      $\mathcal{B}_{\mathbf{m}} \leftarrow \mathbb{F}(\mathbf{x} \odot \mathbf{m}, \gamma_m)$ 
6:      $\mathcal{B}_{\text{mask}} \leftarrow \mathcal{B}_{\text{mask}} \cup \mathcal{B}_{\mathbf{m}}$ 
7:   end for
8:    $\mathcal{B}_{\text{base}} \leftarrow \mathbb{F}(\mathbf{x}, \gamma_b)$ 
9:    $\mathcal{B}_{\text{robust}} \leftarrow \text{BOXPRUNE}(\mathcal{B}_{\text{mask}}, \mathcal{B}_{\text{base}}, \mathbb{S}, \tau)$ 
10:  return  $\mathcal{B}_{\text{robust}}$ 
11: end procedure

12: procedure MASKSET( $k, W, H$ )
13:    $\mathcal{X} = \{ \lceil \frac{W}{k+1} \rceil \cdot t \mid t \in \mathbb{Z}_k^+ \}$ ;  $\mathcal{Y} = \{ \lceil \frac{H}{k+1} \rceil \cdot t \mid t \in \mathbb{Z}_k^+ \}$ 
14:    $\mathcal{M}_{\mathcal{X}} \leftarrow \{ \mathbf{m} \mid \mathbf{m}[i, j] = 0, i \in [0, x); \mathbf{m}[i, j] = 1, i \in [x, W), x \in \mathcal{X} \}$ 
15:    $\mathcal{M}_{\mathcal{Y}} \leftarrow \{ \mathbf{m} \mid \mathbf{m}[i, j] = 0, j \in [0, y); \mathbf{m}[i, j] = 1, j \in [y, H), y \in \mathcal{Y} \}$ 
16:    $\bar{\mathcal{M}}_{\mathcal{X}} \leftarrow \{ \mathbf{1} - \mathbf{m} \mid \mathbf{m} \in \mathcal{M}_{\mathcal{X}} \}$ ;  $\bar{\mathcal{M}}_{\mathcal{Y}} = \{ \mathbf{1} - \mathbf{m} \mid \mathbf{m} \in \mathcal{M}_{\mathcal{Y}} \}$ 
17:   return  $\mathcal{M}_{\mathcal{X}} \cup \mathcal{M}_{\mathcal{Y}} \cup \bar{\mathcal{M}}_{\mathcal{X}} \cup \bar{\mathcal{M}}_{\mathcal{Y}}$ 
18: end procedure

19: procedure BOXPRUNE( $\mathcal{B}_{\text{mask}}, \mathcal{B}_{\text{base}}, \mathbb{S}, \tau$ )
20:    $\mathcal{B}_{\text{mask}}^{\text{filtered}} \leftarrow \{ \mathbf{b}_m \in \mathcal{B}_{\text{mask}} \mid \nexists \mathbf{b}_b \in \mathcal{B}_{\text{base}} : \mathbb{S}(\mathbf{b}_m, \mathbf{b}_b) > \tau \}$ 
21:    $\mathcal{B}_{\text{mask}}^{\text{pruned}} \leftarrow \{ \text{REP}(\hat{\mathcal{B}}, \mathbb{S}) \mid \hat{\mathcal{B}} \in \text{CLUSTER}(\mathcal{B}_{\text{mask}}^{\text{filtered}}, \mathbb{S}) \}$ 
22:    $\mathcal{B}_{\text{robust}} \leftarrow \mathcal{B}_{\text{base}} \cup \mathcal{B}_{\text{mask}}^{\text{pruned}}$ 
23:   return  $\mathcal{B}_{\text{robust}}$ 
24: end procedure

```

---

We use the sub-procedure MASKSET( $\cdot$ ) for the mask set generation. It takes the image size  $W \times H$  and the number of horizontal/vertical lines  $k$  as inputs and outputs a mask set  $\mathcal{M}$  for pixel masking. In this sub-procedure, we first generate two sets of coordinates  $\mathcal{X}, \mathcal{Y}$  for vertical and horizontal lines (Line 13); each set contain  $k$  evenly spaced coordinates. Next, we generate a mask set  $\mathcal{M}_{\mathcal{X}}$ , whose elements mask the left halves of the image (Line 14). Similarly, we generate  $\mathcal{M}_{\mathcal{Y}}$  that masks the lower halves (Line 15),  $\bar{\mathcal{M}}_{\mathcal{X}}$  that masks the right halves (Line 16), and  $\bar{\mathcal{M}}_{\mathcal{Y}}$  that masks the upper halves (Line 16). The final mask set  $\mathcal{M}$  is the union of these four sets (Line 17).

With the generated mask set  $\mathcal{M}$ , we iterate over each mask  $\mathbf{m} \in \mathcal{M}$  (Line 4), perform object detection on the masked image  $\mathbf{x} \odot \mathbf{m}$  (Line 5), and then gather detected boxes into the box set  $\mathcal{B}_{\text{mask}}$  (Line 6). We note that we only consider detected boxes with high prediction confidence via calling  $\mathbb{F}(\cdot, \gamma_m)$ .

This is because object detection becomes less precise when part of the object is masked; using a high confidence threshold  $\gamma_m$  can filter out unconfident and imprecise predicted boxes for better model performance. The next step in ObjectSeeker is to perform secure box pruning on the detected boxes, which will be discussed in the next subsection.

### 3.2 Secure Box Pruning

**Intuition and challenge.** In Section 3.1, our masking strategy aims to ensure that we can safely see most benign pixels/objects from some of the masked images that contain no adversarial pixels. With this robustness property, a naive defense strategy is to take all boxes detected on masked images as the final output. Since the attacker has no influence over the detection results when the patch is completely masked, we will detect most ground-truth objects and achieve a high robust recall against the hiding attack.

However, this approach is not ideal: we will have many duplicate boxes for one object since an object might be detected multiple times in different masked images (see “masked boxes” in Figure 1 for visual examples); redundant duplicate boxes will be considered as false-positive errors and hurt the detection precision. Therefore, we need to further identify and prune these redundant boxes in ObjectSeeker. We note that the box pruning is a non-trivial task since duplicate boxes can look very different (e.g., in Figure 1, some boxes detect the left part of the motorbike while some detect the right part). Moreover, the box pruning should be done in a secure manner since an adaptive attacker might introduce malicious boxes to interfere with the box pruning. Overall, we aim to perform secure box pruning to improve prediction *precision* while preserving the robust *recall* against the patch hiding attack.

**Box pruning algorithm.** The high-level idea of our box pruning is to use a function  $\mathbb{S} : \mathcal{B} \times \mathcal{B} \rightarrow \mathbb{R}$  to robustly measure the similarity between detected boxes so that we can identify and prune redundant boxes. Different similarity score functions can give different robustness bounds and different types of robustness notions. We focus on using IoA as the similarity score for achieving IoA robustness (recall Section 2.3); we will also discuss an alternative choice in Appendix B.

We visualize the pruning algorithm in the right of Figure 1 and present the pseudocode in Line 8-9 and Line 20-22 of Algorithm 1. To start with, we perform one vanilla model prediction on the original unmasked image  $\mathbf{x}$  to obtain the (potentially vulnerable) base detection results  $\mathcal{B}_{\text{base}} = \mathbb{F}(\mathbf{x}, \gamma_b)$  (Line 8).<sup>6</sup> We term boxes detected on the original unmasked image *base boxes* and boxes detected on masked images as *masked boxes*. Then, we call the sub-procedure  $\text{BOXPRUNE}(\mathcal{B}_{\text{mask}}, \mathcal{B}_{\text{base}}, \mathbb{S}, \tau)$  for box pruning, which first *filters* out redundant masked boxes that are duplicates of base

<sup>6</sup>We note that  $\gamma_b$  and  $\gamma_m$  are two separate parameters. We further discuss their difference and relation in Appendix A.

boxes and then *unionizes* unfiltered masked boxes for the final prediction output.

**Box filtering.** The first pruning operation aims to filter out redundant masked boxes that are highly similar to the base boxes (measured by  $\mathbb{S}$ ). Specifically, we calculate the pairwise similarity scores between masked boxes and base boxes and remove masked boxes  $\mathbf{b}_m$  whose similarity with a particular base box  $\mathbf{b}_b$  exceeds a filtering threshold  $\tau$ , i.e.,  $\mathbb{S}(\mathbf{b}_m, \mathbf{b}_b) > \tau$ . This filtering operation is illustrated in Line 20 of Algorithm 1. In the top right of Figure 1, we can see that duplicate boxes are effectively removed when base boxes also detect the object.

**Box unionizing.** If base box predictions are accurate, most masked boxes will be removed during the box filtering operation (top right of Figure 1). However, when a patch hiding attack happens, base box predictions disappear, and thus no masked boxes will be filtered (bottom right of Figure 1). As a result, we need to further prune/unionize the remaining redundant masked boxes. The high-level idea of box unionizing is to use similarity score  $\mathbb{S}$  to cluster similar boxes via  $\text{CLUSTER}(\cdot)$  and output one box representative for each cluster via  $\text{REP}(\cdot)$ . The collection of these boxes representatives is the final *pruned masked boxes*. This process occurs in Line 21 of Algorithm 1 and is illustrated in the bottom right of Figure 1.

**ObjectSeeker output.** After the box filtering and unionizing operations, we combine the pruned masked boxes  $\mathcal{B}_{\text{mask}}^{\text{pruned}}$  with base boxes  $\mathcal{B}_{\text{base}}$  as the final output of ObjectSeeker (Line 23 and Line 10).

**Instantiation with IoA.** In our implementation when we take IoA as  $\mathbb{S}$ , we instantiate  $\text{CLUSTER}(\cdot)$  using a distance-based clustering algorithm DBSCAN [14]. For each box cluster, we generate the box representative as  $\text{REP}(\hat{\mathcal{B}}) = \bigcup_{\mathbf{b} \in \hat{\mathcal{B}}} \mathbf{b}$ , i.e., taking the mathematical union of all boxes as the representative of the cluster. In the rest of this paper, we will refer to this instance of box pruning as **IOA-BOXPRUNE** and call the corresponding ObjectSeeker instance **IOA-OBJECTSEEKER**.

### 3.3 Robustness Certification

So far, we have discussed how to use patch-agnostic masking to neutralize the adversarial patch and how to securely perform box pruning to remove duplicate boxes. In this subsection, we discuss how to certify the robustness of ObjectSeeker for certain objects against any patch hiding attacker within our threat model. Here, we will focus on the case where we implement  $\mathbb{S}$  with IoA for certifiable IoA robustness. However, the high-level idea of certification is similar for different  $\mathbb{S}$ ; we will discuss a different  $\mathbb{S}$  and its certification in Appendix B.

We first formally reiterate our robustness objective.

**Definition 2** (Certifiable IoA robustness). *We consider ObjectSeeker is certifiably IoA-robust for an object  $\mathbf{b}_{gt}$  on an image  $\mathbf{x}$  against a patch attacker  $\mathcal{A}_P$  (discussed in Section 2.2), if we can always predict a box  $\mathbf{b}'$  satisfying*

$\text{IOA}(\mathbf{b}_{gt}, \mathbf{b}') > T$ , where  $T \in [0, 1]$  is a certification threshold. Formally, we have:  $\forall \mathbf{x}' \in \mathcal{A}_p(\mathbf{x}), \exists \mathbf{b}' \in \mathcal{B}_{robust} = \text{IOA-OBJECTSEEKER}(\mathbf{x}') \text{ s.t. } \text{IOA}(\mathbf{b}_{gt}, \mathbf{b}') > T$ .

Next, we discuss the intuition of our certification algorithm and proof.

**Intuition.** In our two-step ObjectSeeker framework, we aim to detect victim objects on *masked images without adversarial pixels* and combine pruned masked boxes and base boxes as the final defense output  $\mathcal{B}_{robust}$ . Intuitively, if we detect a ‘‘good’’ masked box in a masked image without adversarial pixels, this good masked box is likely to ‘‘survive’’ the box pruning procedure and become one good box in  $\mathcal{B}_{robust}$  (the output of IOA-BOXPRUNE and IOA-OBJECTSEEKER). We formally define the property of a ‘‘good’’ box as *pruning-safe masked box* below.

**Definition 3** (pruning-safe masked box). *We call a masked box  $\mathbf{b}_m$  a pruning-safe masked box for a ground-truth object  $\mathbf{b}_{gt}$  and box pruning procedure  $\text{IOA-BOXPRUNE}(\cdot)$  if it ensures that there is always a box  $\mathbf{b}'$  in the box pruning output satisfying  $\text{IOA}(\mathbf{b}_{gt}, \mathbf{b}') > T$ . Formally, we have:  $\forall \mathcal{B}_{mask} \text{ s.t. } \mathbf{b}_m \in \mathcal{B}_{mask}, \forall \mathcal{B}_{base}, \exists \mathbf{b}' \in \mathcal{B}_{robust} = \text{IOA-BOXPRUNE}(\mathcal{B}_{mask}, \mathcal{B}_{base}, \tau) \text{ s.t. } \text{IOA}(\mathbf{b}_{gt}, \mathbf{b}') > T$ .*

We note that this definition considers all possible  $\mathcal{B}_{mask}$  s.t.  $\mathbf{b}_m \in \mathcal{B}_{mask}$  and all possible  $\mathcal{B}_{base}$ . This captures adaptive attackers’ capability to maliciously manipulate some of the masked boxes in  $\mathcal{B}_{mask}$  (when the patch is not removed by the masks) and all base boxes in  $\mathcal{B}_{base}$  to interfere with the box pruning procedure. With the definition of pruning-safe masked boxes, we can derive the following lemma discussing the sufficient conditions of certifiable IoA robustness.

**Lemma 1.** *Given a ground-truth box  $\mathbf{b}_{gt}$ , one patch region  $\mathbf{p}$ , if we can detect a pruning-safe masked box  $\mathbf{b}_m$  from a masked image  $\mathbf{x} \odot \mathbf{m}$  with no adversarial pixels (i.e.,  $\mathbf{m}[i, j] \leq \mathbf{p}[i, j], \forall (i, j)$ ), IOA-OBJECTSEEKER has certifiable IoA robustness for the object  $\mathbf{b}_{gt}$  against the attacker  $\mathcal{A}_{\{\mathbf{p}\}}$ .*

*Proof.* Since the pruning-safe masked box  $\mathbf{b}_m$  is detected from a masked image without adversarial pixels, we have  $\mathbf{b}_m \in \mathcal{B}_{mask}$  in no matter what a patch attacker does using  $\mathbf{p}$ . From the definition of pruning-safe mask box, we have the guarantee that  $\exists \mathbf{b}' \in \mathcal{B}_{robust} \text{ s.t. } \text{IOA}(\mathbf{b}_{gt}, \mathbf{b}') > T$ , which implies certifiable IoA robustness.  $\square$

With Lemma 1, an IoA robustness certification procedure only needs to look for pruning-safe masked boxes detected on masked images without adversarial pixels. Next, we will present two lemmas discussing how to identify pruning-safe masked boxes.

Recall that the box pruning involves two steps of box filtering (Line 20 of Algorithm 1) and box unionizing (Line 21 of Algorithm 1). Lemma 2 will give a lower bound of the IoA guarantee for the first step (box filtering). Lemma 3 will use

this lower bound to further derive the sufficient condition of being a pruning-safe masked box for the entire box pruning procedure (box filtering and box unionizing).

**Lemma 2.** *For any ground-truth object box  $\mathbf{b}_{gt}$ , detected masked box  $\mathbf{b}_m$ , and box  $\mathbf{b}_b$  with  $\text{IOA}(\mathbf{b}_m, \mathbf{b}_b) > \tau$ ,<sup>7</sup> we have:*

$$\text{IOA}(\mathbf{b}_{gt}, \mathbf{b}_b) > \frac{|\mathbf{b}_m| \cdot \tau - |\mathbf{b}_m \setminus \mathbf{b}_{gt}|}{|\mathbf{b}_{gt}|}, \forall \mathbf{b}_b \text{ s.t. } \text{IOA}(\mathbf{b}_m, \mathbf{b}_b) > \tau$$

*Proof.* From  $\text{IOA}(\mathbf{b}_m, \mathbf{b}_b) = |\mathbf{b}_m \cap \mathbf{b}_b| / |\mathbf{b}_m| > \tau$ , we have  $|\mathbf{b}_m \cap \mathbf{b}_b| > |\mathbf{b}_m| \cdot \tau$ . With this condition, we can derive an inequality as follows:  $|\mathbf{b}_{gt} \cap \mathbf{b}_b| = |(\mathbf{b}_{gt} \cap \mathbf{b}_b) \cap \mathbf{b}_m| + |(\mathbf{b}_{gt} \cap \mathbf{b}_b) \setminus \mathbf{b}_m| \geq |\mathbf{b}_m \cap \mathbf{b}_b \cap \mathbf{b}_{gt}| = |\mathbf{b}_m \cap \mathbf{b}_b| - |(\mathbf{b}_m \cap \mathbf{b}_b) \setminus \mathbf{b}_{gt}| \geq |\mathbf{b}_m \cap \mathbf{b}_b| - |\mathbf{b}_m \setminus \mathbf{b}_{gt}| > \mathbf{b}_m \cdot \tau - |\mathbf{b}_m \setminus \mathbf{b}_{gt}|$  (two equal signs are based on basic set operations). Finally, we have  $\text{IOA}(\mathbf{b}_{gt}, \mathbf{b}_b) = |\mathbf{b}_{gt} \cap \mathbf{b}_b| / |\mathbf{b}_{gt}| > (|\mathbf{b}_m| \cdot \tau - |\mathbf{b}_m \setminus \mathbf{b}_{gt}|) / |\mathbf{b}_{gt}|$ .  $\square$

We use  $\mathbb{L}_{\text{IOA}}(\mathbf{b}_{gt}, \mathbf{b}_m, \tau) = (|\mathbf{b}_m| \cdot \tau - |\mathbf{b}_m \setminus \mathbf{b}_{gt}|) / |\mathbf{b}_{gt}|$  to denote this lower bound. Lemma 3 will further demonstrate that  $\mathbb{L}_{\text{IOA}} > T$  is the sufficient condition of being a pruning-safe masked box.

**Lemma 3.** *Given a ground-truth object  $\mathbf{b}_{gt}$  and the box filtering threshold  $\tau$ , if there is one masked box  $\mathbf{b}_m \in \mathcal{B}_{mask}$  satisfying that  $\mathbb{L}_{\text{IOA}}(\mathbf{b}_{gt}, \mathbf{b}_m, \tau) > T$ , this box is a pruning-safe masked box for object  $\mathbf{b}_{gt}$  and IOA-BOXPRUNE.*

*Proof.* The detected masked box  $\mathbf{b}_m \in \mathcal{B}_{mask}$  will go through box filtering and box unionizing to generate the final output. We will demonstrate that this masked box  $\mathbf{b}_m$  will ‘‘survive’’ these two operations and become part of the final output, ensuring the IoA robustness.

*Box filtering.* Recall that, in Line 20 of Algorithm 1, we remove a box  $\mathbf{b}_m$  if there is another box  $\mathbf{b}_b \in \mathcal{B}_{base}$  satisfying  $\text{IOA}(\mathbf{b}_m, \mathbf{b}_b) > \tau$ , and the masked box set  $\mathcal{B}_{mask}$  becomes  $\mathcal{B}_{mask}^{\text{filtered}}$  after the filtering. We can prove that there is always a box  $\mathbf{b}^* \in \mathcal{B}_{mask}^{\text{filtered}} \cup \mathcal{B}_{base}$  such that  $\text{IOA}(\mathbf{b}_{gt}, \mathbf{b}^*) > T$ . There are two possible scenarios.

1. If  $\mathbf{b}_m$  is not filtered, we will know there is a box  $\mathbf{b}^* = \mathbf{b}_m \in \mathcal{B}_{mask}^{\text{filtered}}$  such that  $\text{IOA}(\mathbf{b}_{gt}, \mathbf{b}^*) = |\mathbf{b}_{gt} \cap \mathbf{b}_m| / |\mathbf{b}_{gt}| = (|\mathbf{b}_m| - |\mathbf{b}_m \setminus \mathbf{b}_{gt}|) / |\mathbf{b}_{gt}| \geq \mathbb{L}_{\text{IOA}}(\mathbf{b}_{gt}, \mathbf{b}_m, \tau) > T$ .
2. If  $\mathbf{b}_m$  is filtered, there is a box  $\mathbf{b}^* \in \mathcal{B}_{base}$  such that  $\text{IOA}(\mathbf{b}_m, \mathbf{b}^*) > \tau$ . From Lemma 2, we know that this box  $\mathbf{b}^* \in \mathcal{B}_{base}$  satisfies  $\text{IOA}(\mathbf{b}_{gt}, \mathbf{b}^*) > \mathbb{L}_{\text{IOA}}(\mathbf{b}_{gt}, \mathbf{b}_m, \tau) > T$ .

*Box unionizing.* Recall that we will perform clustering over filtered masked boxes  $\mathcal{B}_{mask}^{\text{filtered}}$  and take the mathematical union of each clusters of boxes as the representative of each cluster to get  $\mathcal{B}_{mask}^{\text{pruned}}$  (Line 21 of Algorithm 1). Since the mathematical union operation will not decrease IoA, we know that there is a box  $\mathbf{b}' \in \mathcal{B}_{mask}^{\text{pruned}} \cup \mathcal{B}_{base} = \mathcal{B}_{robust}$  such that  $\text{IOA}(\mathbf{b}_{gt}, \mathbf{b}') \geq \text{IOA}(\mathbf{b}_{gt}, \mathbf{b}^*) > T$ , which implies the certifiable robustness for the object  $\mathbf{b}_{gt}$ .  $\square$

<sup>7</sup>  $\mathbf{b}_b$  will remove  $\mathbf{b}_m$  during the box filtering process given this condition.

---

**Algorithm 2** Certification algorithm for IoA robustness

---

**Input:** Image  $\mathbf{x}$ , the object (bounding box)  $\mathbf{b}_{\text{gt}}$  to be certified, valid patch region set  $\mathcal{P}$ , defense setup  $(\mathbb{F}, \mathcal{M}, \gamma_m, \tau)$ , certification threshold  $T$ .

**Output:** Whether  $\mathbf{b}_{\text{gt}}$  has certifiable IoA robustness

```
1: procedure CERTIFY( $\mathbf{x}, \mathbf{b}, \mathcal{P}, \mathbb{F}, \mathcal{M}, \gamma_m, \tau$ )
2:   for  $\mathbf{p} \in \mathcal{P}$  do
3:      $f_{\mathbf{p}} \leftarrow \text{False}$ 
4:     for  $\mathbf{m} \in \{\mathbf{m} \in \mathcal{M} \mid \mathbf{m}[i, j] \leq \mathbf{p}[i, j], \forall(i, j)\}$  do
5:        $\mathcal{B}_{\mathbf{m}} \leftarrow \mathbb{F}(\mathbf{x} \odot \mathbf{m}, \gamma_m)$ 
6:       if  $\exists \mathbf{b}_{\mathbf{m}} \in \mathcal{B}_{\mathbf{m}}$  s.t.  $\mathbb{L}_{\text{IoA}}(\mathbf{b}_{\text{gt}}, \mathbf{b}_{\mathbf{m}}, \tau) > T$  then
7:          $f_{\mathbf{p}} \leftarrow \text{True}$ ; break
8:       end if
9:     end for
10:    if  $f_{\mathbf{p}} = \text{False}$  then
11:      return  $\text{False}$ 
12:    end if
13:  end for
14:  return  $\text{True}$ 
15: end procedure
```

---

**Robustness certification.** Lemma 1 and Lemma 3 together provide a simple way to certify IoA robustness: if we can detect a masked box  $\mathbf{b}_{\mathbf{m}}$  on a masked image with no adversarial pixel ( $\mathbf{m}[i, j] \leq \mathbf{p}[i, j], \forall(i, j)$ ), and this box is pruning-safe ( $\mathbb{L}_{\text{IoA}} > T$ ), we have certifiable IoA robustness for the object  $\mathbf{b}_{\text{gt}}$  against the patch region  $\mathbf{p}$ . Then, we can easily design a robustness certification procedure in Algorithm 2 by checking these conditions against all possible patch region  $\mathbf{p} \in \mathcal{P}$ . We state the correctness of Algorithm 2 in the following theorem and discuss the certification details in the proof.

**Theorem 1.** *Given a ground-truth object box  $\mathbf{b}_{\text{gt}}$  in the input image  $\mathbf{x}$ , defense setup  $(\mathbb{F}, \mathcal{M}, \gamma_m, \tau)$ , certification threshold  $T$ , and a set of valid patch regions  $\mathcal{P}$ , if Algorithm 2 returns  $\text{True}$ , IOA-OBJECTSEEKER has certifiable IoA robustness for the object  $\mathbf{b}_{\text{gt}}$  against any attacker in  $\mathcal{A}_{\mathcal{P}}$ .*

*Proof.* The certification algorithm will iterate every valid patch region  $\mathbf{p} \in \mathcal{P}$  to determine if ObjectSeeker can certify the robustness for the ground-truth object  $\mathbf{b}_{\text{gt}}$  against each  $\mathbf{p}$  (Line 3-9). If the certification procedure finds any  $\mathbf{p}$  that might bypass ObjectSeeker, the certification fails and returns  $\text{False}$  (Line 11); otherwise, it returns  $\text{True}$  (Line 14), indicating that ObjectSeeker is robust for  $\mathbf{b}_{\text{gt}}$  against any attacker within the threat model  $\mathcal{A}_{\mathcal{P}}$  (defined in Section 2.2).

For each patch region  $\mathbf{p}$ , we initialize the robustness flag  $f_{\mathbf{p}}$  to  $\text{False}$  (Line 3). Next, we will examine every mask  $\mathbf{m} \in \mathcal{M}$  that can remove the entire patch (i.e.,  $\mathbf{m}[i, j] \leq \mathbf{p}[i, j], \forall(i, j)$ ). For each mask  $\mathbf{m}$ , we perform object detection on the masked image  $\mathbf{x} \odot \mathbf{m}$  to get masked boxes  $\mathcal{B}_{\mathbf{m}}$  (Line 5). If we can find a masked box  $\mathbf{b}_{\mathbf{m}} \in \mathcal{B}_{\mathbf{m}}$  such that  $\mathbb{L}_{\text{IoA}}(\mathbf{b}_{\text{gt}}, \mathbf{b}_{\mathbf{m}}, \tau) > T$ , we can certify the robustness for this object  $\mathbf{b}_{\text{gt}}$  against this  $\mathbf{p}$  based on Lemma 1 and Lemma 3 (Line 6-7). On the other

hand, if we try all possible masks that can remove the patch, but the condition is never satisfied, the ground-truth object  $\mathbf{b}_{\text{gt}}$  might be vulnerable to this patch  $\mathbf{p}$  and the certification procedure returns  $\text{False}$  (Line 11).

Finally, if the certification algorithm enumerates every valid patch  $\mathbf{p} \in \mathcal{P}$  and does not return  $\text{False}$ , it implies that ObjectSeeker has certified robustness for the object  $\mathbf{b}_{\text{gt}}$  against all possible  $\mathbf{p}$  within the threat model. The algorithm returns  $\text{True}$  (Line 14).  $\square$

Algorithm 2 and Theorem 1 allow us to determine the certifiable robustness of ObjectSeeker for an object in a given image. In our evaluation, we will report the fraction of certified objects in the annotated test set of benchmark datasets as the robustness metric.

## 4 Evaluation

In this section, we implement ObjectSeeker with two vanilla object detectors and evaluate the defense performance on two object detection datasets (we include a third additional dataset in Appendix E). We demonstrate a significant robustness improvement ( $\sim 10\%$ - $40\%$  absolute and  $\sim 2$ - $6\times$  relative) over the prior work DetectorGuard [68] as well as similarly high clean performance ( $\sim 1\%$  drop compared with vanilla undefended models). We will release our source code for reproducibility.

### 4.1 Setup

In this subsection, we introduce our evaluation setup: datasets, object detectors, evaluation metrics, and defense setups.

#### Datasets.

**VOC [15].** The detection challenge of the PASCAL Visual Object Classes (VOC) project has annotations for 20 different objects classes. We combine the `trainval2007` set (5k images) and the `trainval2012` set (11k images) for training and evaluate ObjectSeeker on the `test2007` set (5k images), which is a conventional usage of the PASCAL VOC dataset [33, 74].

**COCO [30].** The Microsoft Common Objects in Context (COCO) dataset is a challenging object detection dataset with 80 annotated object classes. We use the `COCO2017` split for training (117k images) and validation (5k images).

#### Object detectors.

**YOLO-R [62]** is the state-of-the-art one-stage object detector that achieves a good balance between inference speed and accuracy. We choose YOLOR-S [62] as the base object detector in ObjectSeeker.

**Swin Transformer [35]** adopts the representative two-stage detector Mask R-CNN [22] architecture and uses the Swin Transformer [35] as the backbone. Its largest model achieves state-of-the-art detection performance on COCO. We choose Swin-S for our experiments.

### Evaluation metrics.

**Average Precision (AP).** We use AP as our evaluation metric for clean performance, which follows object detection benchmark competitions [15, 30] and relevant research papers [4, 22, 22, 29, 33, 51–53, 59, 62]. As we change the confidence threshold  $\gamma$ , the object detector will have different precision and recall values. AP is defined as the average of precision values at different recalls. Intuitively, AP considers the model behavior at different confidence thresholds and provides a view of the model’s overall performance. In our evaluation, we report  $AP_{0.5}$  (AP evaluated with an IoU threshold of 0.5). We provide more details of the AP calculation in Appendix A.

**Certified Recall (CertR).** We use *certified recall* to evaluate defense robustness against patch hiding attacks. The certified recall is defined as the fraction of ground-truth *objects* whose IoA robustness can be certified by our defense (for which Algorithm 2 returns True). We note that the certified recall changes as the *clean* recall of the object detector changes (when we use a different confidence threshold  $\gamma$ ). To enable a fair comparison, we report certified recall at a particular clean recall (CertR@0.x). We report CertR@0.8 for VOC and CertR@0.6 for COCO.

**Robustness evaluation setup.** To evaluate the robustness of ObjectSeeker, we choose a square patch that takes 1% of the image pixels. We consider three patch location threat models: *far-patch* when the patch is far away from the object, *close-patch* when the patch is close to the object, and *over-patch* when the patch overlaps with the object. We will report certified recalls for three different location models with a certification threshold  $T = 0$  to have a fair comparison with DetectorGuard [68]. We will also analyze defense performance when we use different patch sizes, patch shapes, and large certification thresholds  $T$  in Section 4.3. We provide additional details of this evaluation setup in Appendix A.

*Note 1: the patch-agnostic property.* We note that ObjectSeeker is agnostic to the shape, size, and location of the adversarial patch; the specified patch information is only used for robustness evaluation. In other words, our robust detection algorithm and setup do not change when we consider a different patch shape, size, or location, though the robustness performance can change for different patches.

*Note 2: no need for implementing empirical attacks.* We further note that the robustness certification (Algorithm 2) has accounted for all possible attackers within the threat model (recall Theorem 1); thus, *we do not need to consider any empirical adaptive attack for robustness evaluation.*

**Defense parameters.** In our default setting, we set the number of vertical/horizontal lines  $k = 30$  and the filtering threshold  $\tau = 0.6$ . We use different confidence thresholds  $\gamma_b, \gamma_m$  to adjust the *clean recall* of ObjectSeeker for AP and CertR@0.x evaluation; we provide additional details in Appendix A. We note that we choose these parameters because they can give similarly small clean performance drops ( $\sim 1\%$ )

compared with undefended models. We will further analyze the impact of different defense parameters in Section 4.3.

We also implement the DetectorGuard [68] defense for a performance comparison. The setup for DetectorGuard generally follows its original paper [68]; the only differences are that we use YOLOR and Swin as its vanilla object detectors and adjust its binarization thresholds to achieve similarly high clean performance for a fair robustness comparison. We further report false alert rate (FAR) for DetectorGuard since it is an attack-detection defense. FAR is the fraction of clean images for which DetectorGuard issues a false alert. Note that ObjectSeeker is alert-free so it always has a zero FAR.

## 4.2 State-of-the-art Performance of ObjectSeeker

In Table 2, we report the defense performance of ObjectSeeker and compare it with DetectorGuard [68]. We note that ObjectSeeker is able to certify the correct class label of the detected box (in addition to detecting the object); in contrast, DetectorGuard has no guarantee for the label. To enable a fair comparison, we additionally report performance for a variant of ObjectSeeker that ignores the class labels in the step of secure box pruning. We also include the AP metric of vanilla undefended models to understand the clean performance of defenses.

**ObjectSeeker achieves high certified recall across different datasets and threat models.** Table 2 demonstrates that ObjectSeeker achieves high certified recalls. For example, ObjectSeeker-Swin (certify class) achieves a 68.0% certified recall for the far-patch model on the VOC dataset. That is, for 68.0% of the objects in the test set of the VOC dataset, no patch hiding attacker using a 1%-pixel square patch that is far away from the object can bypass our defense (i.e., hide the object). We can also see similarly high numbers across different object detectors, datasets, and threat models.

**ObjectSeeker has a similarly high clean performance as vanilla object detectors.** Comparing APs of vanilla models and ObjectSeeker in Table 2, we can see that ObjectSeeker achieves a similar clean AP as the vanilla object detectors – the AP drops are only  $\sim 1\%$ . The high clean performance can foster the real-world deployment of our defense. We note that the clean performance of ObjectSeeker that certifies class labels is slightly worse than that without class certification. This is because the vanilla object detector can make mistakes between similar object classes (e.g., motorbike vs. bicycle, car vs. bus) when the object is partially masked. Despite the small clean AP drop, we note that ObjectSeeker achieves a stronger robustness notion by certifying class labels.

**ObjectSeeker achieves significant improvements in defense performance compared with DetectorGuard [68].** We also compare defense performance between ObjectSeeker and DetectorGuard [68]. First, we can see that ObjectSeeker achieves a significant improvement in certified recalls. For

Table 2: Performance of vanilla undefended models, ObjectSeeker, and DetectorGuard [68]

Dataset		PASCAL VOC [15]						MS COCO [30]				
Model	Metric	Certify class?	AP <sub>0.5</sub>	FAR	Certified recall (@0.8)			AP <sub>0.5</sub>	FAR	Certified recall (@0.6)		
					far-patch	close-patch	over-patch			far-patch	close-patch	over-patch
YOLOR [62]	Vanilla (undefended)	–	94.3%	–	–	–	–	70.3%	–	–	–	–
	ObjectSeeker	✓	92.9%	–	58.9%	46.7%	18.0%	69.3%	–	41.5%	28.8%	15.5%
	ObjectSeeker	✗	93.2%	–	61.9%	49.8%	21.5%	69.8%	–	44.6%	31.8%	18.1%
	DetectorGuard [68]	✗	93.0%	5.2%	32.7%	25.1%	12.0%	69.6%	2.4%	13.7%	8.0%	3.0%
Swin [35]	Vanilla (undefended)	–	94.3%	–	–	–	–	70.3%	–	–	–	–
	ObjectSeeker	✓	92.6%	–	68.0%	55.2%	22.5%	68.9%	–	34.9%	24.8%	11.7%
	ObjectSeeker	✗	92.9%	–	70.8%	58.0%	26.9%	69.2%	–	37.5%	27.4%	14.2%
	DetectorGuard [68]	✗	92.8%	3.6%	31.2%	23.0%	10.4%	69.2%	1.4%	11.4%	6.8%	2.4%

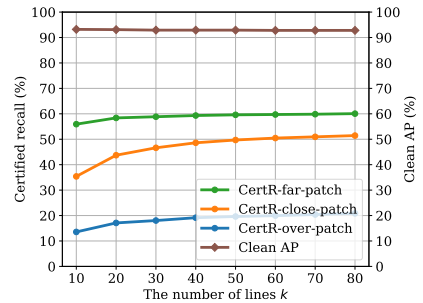
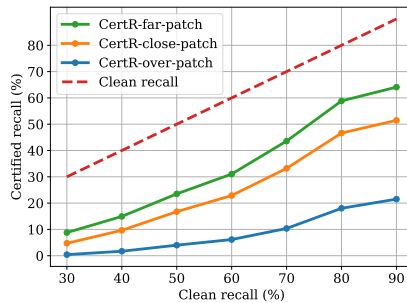
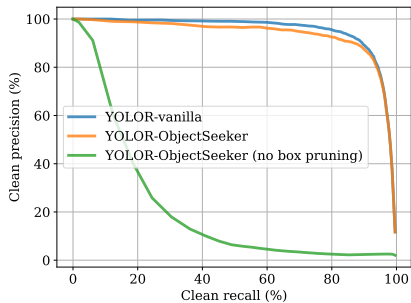


Figure 3: Clean precision vs. clean recall    Figure 4: Certified recall vs. clean recall    Figure 5: Effect of the number of lines  $k$

example, ObjectSeeker-Swin (not certify class) improves the certified recall by  $2\times$  across three different location models on VOC (16.5%-39.6% absolute CertR improvements). The relative improvement on COCO is even larger: ObjectSeeker-YOLOR improves the certified recall by  $6\times$  against the far-patch attacker. We note the significant improvement holds even when we require ObjectSeeker to certify class label: we have achieved much higher certified recalls for an even stronger robustness notion. All these results demonstrate the strength of ObjectSeeker.

Second, ObjectSeeker also has similarly high clean performance as DetectorGuard. When we do not certify class label, ObjectSeeker has slightly higher clean APs than DetectorGuard. When we require ObjectSeeker to protect class labels, the clean APs are slightly lower. Moreover, we want to note that DetectorGuard is an attack-detection defense: it alerts and abstains from making predictions when it detects an attack. This design can cause non-trivial false alerts on the clean images and downgrade the user experience. In contrast, ObjectSeeker is an alert-free defense and thus has more advantages in real-world deployment.

**Summary.** In this subsection, we demonstrate that ObjectSeeker achieves high certified recalls while maintaining high clean APs as vanilla undefended models. Through a comparison with the only prior work DetectorGuard [68], we further demonstrate ObjectSeeker’s state-of-the-art defense performance against patch hiding attacks.

### 4.3 Detailed Analysis of ObjectSeeker

In this subsection, we perform detailed analyses using the YOLOR detector and the VOC dataset. We will report defense performance at different clean recalls, discuss the effect of different defense parameters and patch attacks, and analyze the defense overhead. We report similar analysis results for COCO in Appendix E.

**Clean precision vs. clean recall.** In Figure 3, we plot the clean precision-recall curves for vanilla YOLOR and ObjectSeeker-YOLOR. First, we can see that two curves are close to each other, explaining similar clean APs reported in Table 2. Second, ObjectSeeker-YOLOR has slightly lower precision than vanilla YOLOR when the precision value is higher than 85%; this explains the slight AP drop in Table 2. Third, we additionally plot the curve for ObjectSeeker without the secure box pruning module. We can see that this variant has a very low precision, which demonstrates the necessity and effectiveness of our box pruning module. Finally, we note that the precision of both vanilla YOLOR and ObjectSeeker-YOLOR starts to drop quickly as the clean recall increases over 80%. Therefore, we choose to study model robustness at a clean recall of 0.8 (CertR@0.8) for VOC in Table 2, when the model has both high clean precision and high clean recall.

**Certified recall vs. clean recall.** In Figure 4, we report certified recall at different clean recall values (recall that we only report CertR@0.8 in Table 2). As shown in the figure, the certified recall increases as clean recall increases. This is

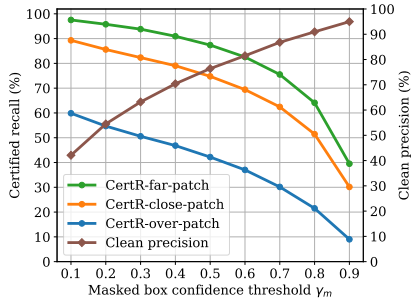


Figure 6: Effect of masked box confidence threshold  $\gamma_m$

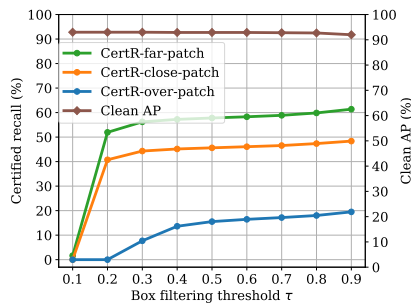


Figure 7: Effect of box filtering threshold  $\tau$

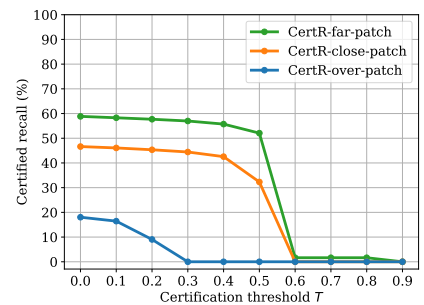


Figure 8: ObjectSeeker performance for different certification thresholds  $T$

expected since the more objects we can detect in the clean setting, the more objects we can try to provide certifiable robustness for. Moreover, we note that the gap between clean recall and certified recall is stable as we vary the clean recall values. This implies that ObjectSeeker is compatible with detectors at different clean recall levels. How to further close this gap is an important future research question.

**Effect of the number of lines  $k$ .** In this analysis, we vary the number of lines  $k$  used for the mask set generation, and plot the defense performance, in terms of clean AP and certified recalls for three location threat models, in Figure 5. As shown in the figure, when we use a larger  $k$ , the robustness (CertR) gradually improves because we have a finer granularity of masks to bound the corrupted image region (recall Figure 2 in Section 3.1). Meanwhile, we can see a slight drop in clean AP as we increase  $k$ . This is because we have more masked images and more masked boxes, which leads to some unsuccessfully pruned boxes and hurts the precision of object detection. Furthermore, we find that the gain in certified robustness becomes minimal when  $k$  is larger than 30. Therefore, we choose  $k = 30$  in our default setting to avoid excessive computational overhead.

**Effect of the masked box confidence threshold  $\gamma_m$ .** In Figure 6, we study the effect of masked box confidence threshold  $\gamma_m$  (with a fixed  $\gamma_b$ ). Recall that we only consider masked boxes whose prediction confidence exceeds the threshold  $\gamma_m$ . Figure 6 demonstrates that the threshold  $\gamma_m$  greatly affects the clean precision and the certified recall of ObjectSeeker. When we use a small threshold  $\gamma_m$ , we have more masked boxes and have a better chance for successful robustness certification. However, a lower threshold leads to less confident and less precise predictions, which finally results in more incorrect boxes and decreases the clean precision.

**Effect of box filtering threshold  $\tau$ .** In Figure 7, we analyze the effect of box filtering threshold  $\tau$ ; we set certification threshold  $T$  to 0.1 (instead of 0) for this analysis. As we use a smaller  $\tau$ , the AP of ObjectSeeker improves since there are fewer boxes left after the box filtering operation. However, the certified robustness is greatly affected with a smaller  $\tau$ . This is because the lower bound proved in Lemma 2 gets lower

with a smaller  $\tau$ , making the robustness certification harder to succeed.

**ObjectSeeker performance for different certification thresholds  $T$ .** In our default setting, we set the certification threshold  $T = 0$ . That is, we consider the defense is robust if we can detect even just a tiny part of the object. This setup follows DetectorGuard [68] and enables a fair comparison in Table 2. Here, we study the defense performance when we require the defense to detect at least  $T$  of the object. We report the results in Figure 8. We can see that the CertR for over-patch is greatly affected by the certification threshold  $T$ . This is because we allow the adversary to place a patch at any location over the object. A worst-case attacker can put the patch at the center of the object to minimize the IoA guarantee. Moreover, we note that there are tiny objects that are even smaller than the patch size [68]. The over-patch attacker can simply occlude the entire object and make the robust object detection impossible. Furthermore, we can see that the robustness for close-patch and far-patch are generally stable until the threshold  $T$  hits a large value. This aligns with our intuition that the localized adversarial patch should only have a malicious effect within a localized region.

**ObjectSeeker performance against different patch sizes.** In Figure 9, we plot the defense performance against patches with different sizes (from 1% to 10% image pixels). As we use a large patch size, the robustness against the over-patch model gradually drops. This is expected since a larger patch has a greater chance to occlude the salient part of the object. Intriguingly, we find that the robustness for close-patch and far-patch exhibits a different behavior: the certified recalls barely change when faced with a larger patch. This analysis further demonstrates that our defense has constrained the adversarial effect to a local region. This property of ObjectSeeker can be helpful in practice when the attacker is not always able to place the patch over the victim object.

**ObjectSeeker performance against different patch shapes.** In this analysis, we study the defense performance against different patch shapes. In Table 3, we report certified recalls for different rectangular shapes that take up 1% of the image pixels (the aspect ratio ranging from 16:1 to 1:16).

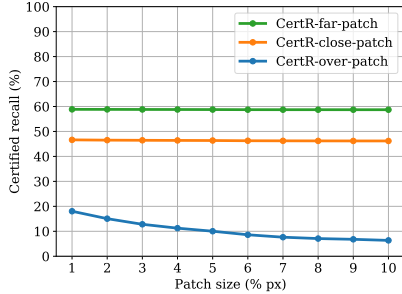


Figure 9: Robustness against different patch sizes

Table 3: Certified recalls (%) against one 1%-pixel patch of different rectangle shapes

aspect ratio	16:1	8:1	4:1	2:1	1:1	1:2	1:4	1:8	1:16
far-patch	58.8	58.8	58.9	58.9	58.9	58.9	58.9	58.9	58.9
close-patch	46.7	46.7	46.7	46.7	46.7	46.7	46.6	46.7	46.7
over-patch	21.3	19.2	19.6	18.8	18.0	18.1	16.8	18.3	18.3

The results demonstrate that ObjectSeeker is effective against different patch shapes: CertRs for far-patch and close-patch barely change; CertRs for over-patch only change slightly. We note that these results are obtained *with the same set of defense parameters*, which further validates the patch-agnostic property of our masking defense.

**Defense overhead.** In Figure 10, we plot the defense overheads (normalized by the runtime of the base vanilla object detector) versus certified recalls for DetectorGuard [68] and ObjectSeeker. As shown in the figure, when the computational budget is small (lower than 20x), DetectorGuard has better robustness (with a small overhead of 2x). However, as we have more computational resources, ObjectSeeker’s performance gradually improves and eventually outperforms DetectorGuard by a large margin. This trade-off between defense overhead and defense performance should be carefully balanced when deploying the ObjectSeeker defense. Moreover, we note that our approach can be trivially parallelized with multiple GPUs (performing vanilla predictions for different masked images simultaneously); in contrast, DetectorGuard’s runtime improvement with multiple GPUs is limited (up to 2x) due to its design.

## 5 Limitation and Future Work

**Robustness against multiple patches.** In this paper, we focus on the setting of *one* adversarial patch of any content, shape, size, and location because it is an unresolved research question. However, we note that the design of ObjectSeeker is general: we only require that some masks from the mask set  $\mathcal{M}$  to can remove all adversarial pixels. If we can design a new mask set that can mask out all (multiple) patches, we can simply plug this new mask set  $\mathcal{M}$  into our ObjectSeeker defense. In Appendix D, we provide a proof-of-concept for

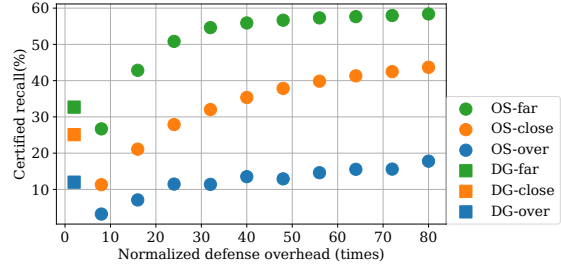


Figure 10: Trade-off between defense overhead and certified robustness (OS: ObjectSeeker; DG: DetectorGuard [68])

ObjectSeeker against two patches, where we use a mask set generated with the knowledge of patch size/shape (not patch-agnostic). We leave further exploration of mask set generation techniques for our future work.

**Improving defense efficiency.** The ObjectSeeker defense needs to perform vanilla object detection on  $4k$  masked images. As analyzed in Figure 5 and Figure 10,  $k$  needs to be large enough to achieve good defense robustness. As a result, the ObjectSeeker defense incurs a non-negligible overhead. How to improve the defense efficiency (e.g., using a more efficient and effective mask set) is an important future research question. Furthermore, we note that for applications whose robustness is important, it is worthwhile to trade defense efficiency for high certifiable robustness. Finally, with the rapid development of computation resources, we expect the defense overhead will be further reduced in the future.

**Further exploration of similarity score functions  $\mathbb{S}$  and robustness notions.** In our ObjectSeeker design, we use a “robust” similarity score function  $\mathbb{S}$  to prune redundant boxes, and we note that using different similarity scores  $\mathbb{S}$  can provide different types of robustness notions. In this paper, we use IoA as the similarity score function  $\mathbb{S}$  and focus on the concept of “IoA robustness” (i.e.,  $\text{IoA}(\mathbf{b}_{\text{gt}}, \mathbf{b}') = |\mathbf{b}_{\text{gt}} \cap \mathbf{b}'| / |\mathbf{b}_{\text{gt}}| > T$ ). This is because IoA captures how much of the ground-truth box is detected and aligns with the objective of defending against patch hiding attacks (following DetectorGuard [68]). However, the IoA robustness does not prevent the model from predicting extremely large boxes for every object (e.g., boxes that cover the entire image have IoA of 1 with any box of the same class). Therefore, one important work direction is to explore different  $\mathbb{S}$  to further constrain the quality of predicted boxes. In Appendix B, we discuss one possible strategy: we use IoU as  $\mathbb{S}$  and achieve “IoU robustness” for far-patch attackers: we aim to predict a box  $\mathbf{b}'$  for each ground-truth box  $\mathbf{b}_{\text{gt}}$  such that  $\text{IoU}(\mathbf{b}_{\text{gt}}, \mathbf{b}') = |\mathbf{b}_{\text{gt}} \cap \mathbf{b}'| / |\mathbf{b}_{\text{gt}} \cup \mathbf{b}'| > T$ . We demonstrate that, against a far-patch attacker, we can achieve certified recall of  $\sim 50\%$  for VOC and  $\sim 40\%$  for COCO with an IoU certification threshold of 0.5. In Appendix C, we further provide a taxonomy of different robustness notions against patch hiding attacks. We hope our discussion on different robustness can inspire stronger certifiably robust defenses

against patch hiding attacks.

## 6 Related Work

**Adversarial patch attacks.** The adversarial patch attack was first introduced for *image classification*. Brown et al. [5] demonstrated that, by constraining all adversarial pixels within a local restricted region, an attacker can carry out the patch attack in the physical world. The physically realizable nature of the patch attack imposed a huge threat to real-world computer vision systems. Follow-up papers further studied variants of patch attacks against image classifiers with different threat models [13, 25, 31, 32, 73].

Numerous patch attacks against *object detection* have been proposed in the past years. Liu et al. [34] proposed the first patch attack against object detectors. Lu et al. [36], Chen et al. [9], Eykholt et al. [16], and Zhao et al. [76] proposed different physical attacks against traffic sign recognition. Thys et al. [60], Xu et al. [71], and Wu et al. [65] studied how to use adversarial patches to evade the person detection. Recently, Hu et al. [23] and Tan et al. [58] propose natural-looking patch hiding attacks against object detectors.

**Defenses against adversarial patches.** To counter the threat of adversarial patch attacks, there have been a large number of heuristic-based image classification defenses proposed in recent years [21, 44, 45, 49, 64]. Unfortunately, many of these defenses are found broken when there is an adaptive attacker who knows about the defense setup [10]. To provide a strong provable robustness guarantee for patch attacks, the research community has proposed a number of certifiably robust defenses [11, 20, 27, 38, 42, 55, 66, 67, 69, 75] for image classification models. In this paper, ObjectSeeker focuses on *securing a harder task of object detection*.

How to secure object detectors is a challenging and understudied research question. Saha et al. [54] studied how to constrain the use of spatial context in YOLOv2 [51] and improved the robustness against a patch at the image corner. Metzzen et al. [40] studied meta-learning techniques to improve model robustness. Ji et al. [24] added adversarial patches to the training dataset and taught the model to detect patches. Liang et al [28] proposed two heuristic-based defenses to detect a patch hiding attack. Chiang et al. [10] designed a defense model to detect and remove the adversarial pixels. Despite their contributions to robust object detection research, these defenses are all based on heuristics and do not have any security guarantee.

In contrast, Xiang et al. [68] proposed DetectorGuard as the only certifiably robust defense against patch hiding attacks, which aimed to provide a robustness guarantee for certain certified objects against any adaptive attacker within the threat model. DetectorGuard designed an objectness explaining strategy to build certifiably robust object detectors using off-the-shelf certifiably robust image classifiers. However, DetectorGuard only achieved a limited certified robustness

(recall Table 2). Xiang et al. [68] pointed out that the bottleneck for the defense performance is the imperfection of existing certifiably robust image classifiers: the incorrect classification outputs from the robust image classifier resulted in a heavy trade-off between robustness and clean performance. Though the imperfection of robust image classifiers has been mitigated since DetectorGuard was published [55, 67], we find these new classifiers too expensive to be used in the costly sliding window operation of DetectorGuard. In this paper, we design ObjectSeeker solely based on vanilla undefended object detectors and easily bypass the bottleneck of imperfect image classifiers. In Section 4, we have demonstrated the significant improvements ( $\sim 2-6\times$ ) in robustness performance over DetectorGuard. Moreover, DetectorGuard is an attack-detection defense that has troublesome false alerts in the clean setting while we design ObjectSeeker as an alert-free defense. Finally, DetectorGuard cannot protect the class labels due to its design limitations while ObjectSeeker achieves high certified robustness for bounding box labels in addition to securing the class label (recall Table 2 in Section 4.2).

**Other adversarial example attacks and defenses.** Adversarial example attacks and defenses for computer vision tasks with different threat models have been extensively studied [2, 3, 8, 12, 18, 19, 26, 37, 39, 41, 43, 46–48, 56, 57, 63, 70, 72]. We focus on the adversarial patch attacks because they are physically-realizable and impose a urgent threat to real-world computer vision systems.

## 7 Conclusion

In this paper, we propose ObjectSeeker as a certifiably robust defense against patch hiding attacks. ObjectSeeker is a two-step defense framework: we first perform patch-agnostic masking to neutralize the adversarial effect (without the knowledge of patch size, shape, and location); we next perform secure box pruning for a precise and robust prediction output. We can prove that for certain objects, ObjectSeeker can always detect the object no matter what an adaptive attacker within the threat model does. Our evaluation demonstrates a significant improvement ( $\sim 10\%-40\%$  absolute and  $\sim 2-6\times$  relative) in certified robustness over the only prior work DetectorGuard [68], as well as the high clean performance of ObjectSeeker ( $\sim 1\%$  performance drops compared with vanilla models). Finally, we discuss the implications of different robustness notions and wish to inspire future research on certifiably robust defenses against patch hiding attacks.

## References

- [1] Anish Athalye, Nicholas Carlini, and David A. Wagner. Obfuscated gradients give a false sense of security: Circumventing defenses to adversarial examples. In *Proceedings of the 35th International Conference on Machine Learning (ICML)*, pages 274–283, 2018.
- [2] Marco Barreno, Blaine Nelson, Anthony D Joseph, and J Doug Tygar. The security of machine learning. *Machine Learning*, 81(2):121–148, 2010.
- [3] Battista Biggio, Igino Corona, Davide Maiorca, Blaine Nelson, Nedim Šrndić, Pavel Laskov, Giorgio Giacinto, and Fabio Roli. Evasion attacks against machine learning at test time. In *ECML PKDD*, pages 387–402. Springer, 2013.
- [4] Alexey Bochkovskiy, Chien-Yao Wang, and Hong-Yuan Mark Liao. Yolov4: Optimal speed and accuracy of object detection. *arXiv preprint arXiv:2004.10934*, 2020.
- [5] Tom B. Brown, Dandelion Mané, Aurko Roy, Martín Abadi, and Justin Gilmer. Adversarial patch. In *Advances in neural information processing systems workshops (NeurIPS Workshops)*, 2017.
- [6] Nicholas Carlini, Anish Athalye, Nicolas Papernot, Wieland Brendel, Jonas Rauber, Dimitris Tsipras, Ian Goodfellow, Aleksander Madry, and Alexey Kurakin. On evaluating adversarial robustness. *arXiv preprint arXiv:1902.06705*, 2019.
- [7] Nicholas Carlini and David A. Wagner. Adversarial examples are not easily detected: Bypassing ten detection methods. In *Proceedings of the 10th ACM Workshop on Artificial Intelligence and Security (AISec@CCS)*, pages 3–14, 2017.
- [8] Nicholas Carlini and David A. Wagner. Towards evaluating the robustness of neural networks. In *2017 IEEE Symposium on Security and Privacy (S&P)*, pages 39–57, 2017.
- [9] Shang-Tse Chen, Cory Cornelius, Jason Martin, and Duen Horng Polo Chau. Shapeshifter: Robust physical adversarial attack on faster r-cnn object detector. In *Joint European Conference on Machine Learning and Knowledge Discovery in Databases*, pages 52–68. Springer, 2018.
- [10] Ping-Han Chiang, Chi-Shen Chan, and Shan-Hung Wu. Adversarial pixel masking: A defense against physical attacks for pre-trained object detectors. In *Proceedings of the 29th ACM International Conference on Multimedia*, pages 1856–1865, 2021.
- [11] Ping-Yeh Chiang, Renkun Ni, Ahmed Abdelkader, Chen Zhu, Christoph Studor, and Tom Goldstein. Certified defenses for adversarial patches. In *8th International Conference on Learning Representations (ICLR)*, 2020.
- [12] Jeremy M. Cohen, Elan Rosenfeld, and J. Zico Kolter. Certified adversarial robustness via randomized smoothing. In *Proceedings of the 36th International Conference on Machine Learning (ICML)*, pages 1310–1320, 2019.
- [13] Bao Gia Doan, Minhui Xue, Shiqing Ma, Ehsan Abbasnejad, and Damith C Ranasinghe. Tnt attacks! universal naturalistic adversarial patches against deep neural network systems. *arXiv preprint arXiv:2111.09999*, 2021.
- [14] Martin Ester, Hans-Peter Kriegel, Jörg Sander, and Xiaowei Xu. A density-based algorithm for discovering clusters in large spatial databases with noise. In *Proceedings of the Second International Conference on Knowledge Discovery and Data Mining (KDD)*, pages 226–231. AAAI Press, 1996.
- [15] Mark Everingham, Luc Van Gool, Christopher K. I. Williams, John M. Winn, and Andrew Zisserman. The pascal visual object classes (VOC) challenge. *International Journal of Computer Vision*, 88(2):303–338, 2010.
- [16] Kevin Eykholt, Ivan Evtimov, Earlene Fernandes, Bo Li, Amir Rahmati, Florian Tramer, Atul Prakash, Tadayoshi Kohno, and Dawn Song. Physical adversarial examples for object detectors. In *12th USENIX Workshop on Offensive Technologies (WOOT 18)*, 2018.
- [17] Andreas Geiger, Philip Lenz, Christoph Stiller, and Raquel Urtasun. Vision meets robotics: The kitti dataset. *The International Journal of Robotics Research*, 32(11):1231–1237, 2013.
- [18] Ian J. Goodfellow, Jonathon Shlens, and Christian Szegedy. Explaining and harnessing adversarial examples. In *3rd International Conference on Learning Representations (ICLR)*, 2015.
- [19] Sven Gowal, Krishnamurthy Dvijotham, Robert Stanforth, Rudy Bunel, Chongli Qin, Jonathan Uesato, Relja Arandjelovic, Timothy Arthur Mann, and Pushmeet Kohli. Scalable verified training for provably robust image classification. In *2019 IEEE/CVF International Conference on Computer Vision (ICCV)*, pages 4841–4850, 2019.
- [20] Husheng Han, Kaidi Xu, Xing Hu, Xiaobing Chen, Ling Liang, Zidong Du, Qi Guo, Yanzhi Wang, and Yunji Chen. Scalecert: Scalable certified defense against adversarial patches with sparse superficial layers. *Advances in Neural Information Processing Systems*, 34, 2021.

- [21] Jamie Hayes. On visible adversarial perturbations & digital watermarking. In *2018 IEEE Conference on Computer Vision and Pattern Recognition Workshops (CVPR Workshops)*, pages 1597–1604, 2018.
- [22] Kaiming He, Georgia Gkioxari, Piotr Dollár, and Ross B. Girshick. Mask R-CNN. In *IEEE International Conference on Computer Vision, (ICCV 2017)*, pages 2980–2988. IEEE Computer Society, 2017.
- [23] Yu-Chih-Tuan Hu, Bo-Han Kung, Daniel Stanley Tan, Jun-Cheng Chen, Kai-Lung Hua, and Wen-Huang Cheng. Naturalistic physical adversarial patch for object detectors. In *Proceedings of the IEEE/CVF International Conference on Computer Vision (ICCV)*, pages 7848–7857, 2021.
- [24] Nan Ji, YanFei Feng, Haidong Xie, Xueshuang Xiang, and Naijin Liu. Adversarial yolo: Defense human detection patch attacks via detecting adversarial patches. *arXiv preprint arXiv:2103.08860*, 2021.
- [25] Danny Karmon, Daniel Zoran, and Yoav Goldberg. LaVAN: Localized and visible adversarial noise. In *Proceedings of the 35th International Conference on Machine Learning (ICML)*, pages 2512–2520, 2018.
- [26] Mathias Lécuyer, Vaggelis Atlidakis, Roxana Geambasu, Daniel Hsu, and Suman Jana. Certified robustness to adversarial examples with differential privacy. In *2019 IEEE Symposium on Security and Privacy (S&P)*, pages 656–672, 2019.
- [27] Alexander Levine and Soheil Feizi. (De)randomized smoothing for certifiable defense against patch attacks. *arXiv preprint arXiv:2002.10733*, 2020.
- [28] Bin Liang, Jiachun Li, and Jianjun Huang. We can always catch you: Detecting adversarial patched objects with or without signature. *arXiv preprint arXiv:2106.05261*, 2021.
- [29] Tsung-Yi Lin, Priya Goyal, Ross B. Girshick, Kaiming He, and Piotr Dollár. Focal loss for dense object detection. In *IEEE International Conference on Computer Vision, (ICCV) 2017*, pages 2999–3007. IEEE Computer Society, 2017.
- [30] Tsung-Yi Lin, Michael Maire, Serge J. Belongie, James Hays, Pietro Perona, Deva Ramanan, Piotr Dollár, and C. Lawrence Zitnick. Microsoft COCO: common objects in context. In *European Conference on Computer Vision (ECCV)*, volume 8693, pages 740–755. Springer, 2014.
- [31] Aishan Liu, Xianglong Liu, Jiaxin Fan, Yuqing Ma, Anlan Zhang, Huiyuan Xie, and Dacheng Tao. Perceptual-sensitive GAN for generating adversarial patches. In *The 33rd AAAI Conference on Artificial Intelligence, (AAAI) 2019*, pages 1028–1035. AAAI Press, 2019.
- [32] Aishan Liu, Jiakai Wang, Xianglong Liu, Bowen Cao, Chongzhi Zhang, and Hang Yu. Bias-based universal adversarial patch attack for automatic check-out. In *European conference on computer vision (ECCV)*, volume 12358, pages 395–410. Springer, 2020.
- [33] Wei Liu, Dragomir Anguelov, Dumitru Erhan, Christian Szegedy, Scott E. Reed, Cheng-Yang Fu, and Alexander C. Berg. SSD: single shot multibox detector. In *European conference on computer vision (ECCV)*, volume 9905, pages 21–37. Springer, 2016.
- [34] Xin Liu, Huanrui Yang, Ziwei Liu, Linghao Song, Yiran Chen, and Hai Li. DPATCH: an adversarial patch attack on object detectors. In *AAAI Conference on Artificial Intelligence Workshop (AAAI workshop) 2019*, volume 2301, 2019.
- [35] Ze Liu, Yutong Lin, Yue Cao, Han Hu, Yixuan Wei, Zheng Zhang, Stephen Lin, and Baining Guo. Swin transformer: Hierarchical vision transformer using shifted windows. In *IEEE/CVF International Conference on Computer Vision (ICCV)*, 2021.
- [36] Jiajun Lu, Hussein Sibai, and Evan Fabry. Adversarial examples that fool detectors. *arXiv preprint arXiv:1712.02494*, 2017.
- [37] Aleksander Madry, Aleksandar Makelov, Ludwig Schmidt, Dimitris Tsipras, and Adrian Vladu. Towards deep learning models resistant to adversarial attacks. In *6th International Conference on Learning Representations (ICLR)*, 2018.
- [38] Michael McCoyd, Won Park, Steven Chen, Neil Shah, Ryan Roggenkemper, Minjune Hwang, Jason Xinyu Liu, and David A. Wagner. Minority reports defense: Defending against adversarial patches. In *Applied Cryptography and Network Security Workshops (ACNS Workshops)*, volume 12418, pages 564–582. Springer, 2020.
- [39] Dongyu Meng and Hao Chen. Magnet: A two-pronged defense against adversarial examples. In *Proceedings of the 2017 ACM SIGSAC Conference on Computer and Communications Security (CCS)*, pages 135–147, 2017.
- [40] Jan Hendrik Metzen, Nicole Finnie, and Robin Huttmacher. Meta adversarial training against universal patches. In *ICML 2021 Workshop on Adversarial Machine Learning*, 2021.
- [41] Jan Hendrik Metzen, Tim Genewein, Volker Fischer, and Bastian Bischoff. On detecting adversarial perturbations. In *5th International Conference on Learning Representations (ICLR)*, 2017.

- [42] Jan Hendrik Metzen and Maksym Yatsura. Efficient certified defenses against patch attacks on image classifiers. In *9th International Conference on Learning Representations (ICLR)*, 2021.
- [43] Matthew Mirman, Timon Gehr, and Martin T. Vechev. Differentiable abstract interpretation for provably robust neural networks. In *Proceedings of the 35th International Conference on Machine Learning (ICML)*, pages 3575–3583, 2018.
- [44] Norman Mu and David Wagner. Defending against adversarial patches with robust self-attention. In *ICML 2021 Workshop on Uncertainty and Robustness in Deep Learning*, 2021.
- [45] Muzammal Naseer, Salman Khan, and Fatih Porikli. Local gradients smoothing: Defense against localized adversarial attacks. In *IEEE Winter Conference on Applications of Computer Vision (WACV)*, pages 1300–1307, 2019.
- [46] Nicolas Papernot, Patrick D. McDaniel, Somesh Jha, Matt Fredrikson, Z. Berkay Celik, and Ananthram Swami. The limitations of deep learning in adversarial settings. In *IEEE European Symposium on Security and Privacy (EuroS&P)*, pages 372–387, 2016.
- [47] Nicolas Papernot, Patrick D. McDaniel, Xi Wu, Somesh Jha, and Ananthram Swami. Distillation as a defense to adversarial perturbations against deep neural networks. In *IEEE Symposium on Security and Privacy (S&P)*, pages 582–597, 2016.
- [48] Aditi Raghunathan, Jacob Steinhardt, and Percy Liang. Certified defenses against adversarial examples. In *6th International Conference on Learning Representations (ICLR)*, 2018.
- [49] Sukrut Rao, David Stutz, and Bernt Schiele. Adversarial training against location-optimized adversarial patches. In *ECCV Workshops*, 2020.
- [50] Joseph Redmon, Santosh Divvala, Ross Girshick, and Ali Farhadi. You only look once: Unified, real-time object detection. In *Proceedings of the IEEE conference on computer vision and pattern recognition*, pages 779–788, 2016.
- [51] Joseph Redmon and Ali Farhadi. Yolo9000: better, faster, stronger. In *Proceedings of the IEEE conference on computer vision and pattern recognition*, pages 7263–7271, 2017.
- [52] Joseph Redmon and Ali Farhadi. Yolov3: An incremental improvement. *arXiv preprint arXiv:1804.02767*, 2018.
- [53] Shaoqing Ren, Kaiming He, Ross Girshick, and Jian Sun. Faster r-cnn: Towards real-time object detection with region proposal networks. In *Advances in neural information processing systems*, pages 91–99, 2015.
- [54] Aniruddha Saha, Akshayvarun Subramanya, Koninika Patil, and Hamed Pirsiavash. Role of spatial context in adversarial robustness for object detection. In *Proceedings of the IEEE/CVF Conference on Computer Vision and Pattern Recognition Workshops (CVPR Workshops)*, pages 784–785, 2020.
- [55] Hadi Salman, Saachi Jain, Eric Wong, and Aleksander Mądry. Certified patch robustness via smoothed vision transformers. *arXiv preprint arXiv:2110.07719*, 2021.
- [56] Hadi Salman, Jerry Li, Ilya P. Razenshteyn, Pengchuan Zhang, Huan Zhang, Sébastien Bubeck, and Greg Yang. Provably robust deep learning via adversarially trained smoothed classifiers. In *Conference on Neural Information Processing Systems (NeurIPS)*, pages 11289–11300, 2019.
- [57] Christian Szegedy, Wojciech Zaremba, Ilya Sutskever, Joan Bruna, Dumitru Erhan, Ian J. Goodfellow, and Rob Fergus. Intriguing properties of neural networks. In *2nd International Conference on Learning Representations (ICLR)*, 2014.
- [58] Jia Tan, Nan Ji, Haidong Xie, and Xueshuang Xiang. Legitimate adversarial patches: Evading human eyes and detection models in the physical world. In *Proceedings of the 29th ACM International Conference on Multimedia*, pages 5307–5315, 2021.
- [59] Mingxing Tan, Ruoming Pang, and Quoc V Le. Efficientdet: Scalable and efficient object detection. In *2020 IEEE/CVF Conference on Computer Vision and Pattern Recognition (CVPR 2020)*, pages 10781–10790, 2020.
- [60] Simen Thys, Wiebe Van Ranst, and Toon Goedemé. Fooling automated surveillance cameras: adversarial patches to attack person detection. In *Proceedings of the IEEE Conference on Computer Vision and Pattern Recognition Workshops*, 2019.
- [61] Florian Tramer, Nicholas Carlini, Wieland Brendel, and Aleksander Madry. On adaptive attacks to adversarial example defenses. *arXiv preprint arXiv:2002.08347*, 2020.
- [62] Chien-Yao Wang, I-Hau Yeh, and Hong-Yuan Mark Liao. You only learn one representation: Unified network for multiple tasks. *arXiv preprint arXiv:2105.04206*, 2021.

- [63] Eric Wong and J. Zico Kolter. Provable defenses against adversarial examples via the convex outer adversarial polytope. In *Proceedings of the 35th International Conference on Machine Learning (ICML)*, pages 5283–5292, 2018.
- [64] Tong Wu, Liang Tong, and Yevgeniy Vorobeychik. Defending against physically realizable attacks on image classification. In *ICLR*, 2020.
- [65] Zuxuan Wu, Ser-Nam Lim, Larry S. Davis, and Tom Goldstein. Making an invisibility cloak: Real world adversarial attacks on object detectors. In *European Conference on Computer Vision (ECCV) 2020*, volume 12349, pages 1–17, 2020.
- [66] Chong Xiang, Arjun Nitin Bhagoji, Vikash Sehwal, and Prateek Mittal. Patchguard: A provably robust defense against adversarial patches via small receptive fields and masking. In *30th USENIX Security Symposium (USENIX Security)*, 2021.
- [67] Chong Xiang, Saeed Mahloujifar, and Prateek Mittal. Patchcleanser: Certifiably robust defense against adversarial patches for any image classifier. *arXiv preprint arXiv:2108.09135*, 2021.
- [68] Chong Xiang and Prateek Mittal. Detectorguard: Provably securing object detectors against localized patch hiding attacks. In *ACM SIGSAC Conference on Computer and Communications Security (CCS)*. ACM, 2021.
- [69] Chong Xiang and Prateek Mittal. Patchguard++: Efficient provable attack detection against adversarial patches. In *ICLR 2021 Workshop on Security and Safety in Machine Learning Systems*, 2021.
- [70] Chong Xiang, Charles R Qi, and Bo Li. Generating 3d adversarial point clouds. In *IEEE/CVF Conference on Computer Vision and Pattern Recognition (CVPR)*, pages 9136–9144, 2019.
- [71] Kaidi Xu, Gaoyuan Zhang, Sijia Liu, Quanfu Fan, Mengshu Sun, Hongge Chen, Pin-Yu Chen, Yanzhi Wang, and Xue Lin. Adversarial t-shirt! evading person detectors in a physical world. In *European Conference on Computer Vision (ECCV) 2020*, volume 12350, pages 665–681, 2020.
- [72] Weilin Xu, David Evans, and Yanjun Qi. Feature squeezing: Detecting adversarial examples in deep neural networks. In *25th Annual Network and Distributed System Security Symposium (NDSS)*, 2018.
- [73] Chenglin Yang, Adam Kortylewski, Cihang Xie, Yinzhi Cao, and Alan Yuille. Patchattack: A black-box texture-based attack with reinforcement learning. In *European Conference on Computer Vision (ECCV)*, pages 681–698, 2020.
- [74] Haichao Zhang and Jianyu Wang. Towards adversarially robust object detection. In *2019 IEEE/CVF International Conference on Computer Vision (ICCV) 2019*, pages 421–430. IEEE, 2019.
- [75] Zhanyuan Zhang, Benson Yuan, Michael McCoyd, and David Wagner. Clipped bagnet: Defending against sticker attacks with clipped bag-of-features. In *3rd Deep Learning and Security Workshop (DLS)*, 2020.
- [76] Yue Zhao, Hong Zhu, Ruigang Liang, Qintao Shen, Shengzhi Zhang, and Kai Chen. Seeing isn’t believing: Towards more robust adversarial attack against real world object detectors. In *Proceedings of the 2019 ACM SIGSAC Conference on Computer and Communications Security*, pages 1989–2004, 2019.

## A Additional Details of Implementation and Evaluation

**AP in conventional object detection research.** As discussed in Section 4.1, different confidence thresholds would give different precision and recall for an object detector; thus, it is not representative enough to simply evaluate model performance at one fixed confidence threshold. To overcome this challenge, conventional object detection research uses Average Precision (AP) as the main evaluation metric: we vary the confidence threshold from zero to one, record the precision-recall pairs at different thresholds, and finally calculate AP as the averaged precision value across different recall values. AP can also be considered as the Area under Curve (AUC) of the precision-recall curve and thus provides a global view of the model performance. Furthermore, note that we consider a detected box a true-positive only when its IoU with the ground-truth box exceeds a certain threshold, and TP is used for calculating precision and recall. In our evaluation, we set this IoU threshold to 0.5 and report  $AP_{0.5}$ .

**Confidence thresholds and AP calculation in ObjectSeeker.** As presented in Algorithm 1, we only consider boxes whose confidence values exceed certain thresholds; we have two separate confidence thresholds  $\gamma_m, \gamma_b$  for masked boxes and base boxes, respectively. Here, we provide additional implementation details and insights of this design.

In our implementation of ObjectSeeker, we set the masked box threshold  $\gamma_m$  as a function of the base box threshold  $\gamma_b$ . Specifically, we have  $\gamma_m = \max(\alpha, \gamma_b + (1 - \gamma_b) \cdot \beta)$ ,  $\alpha, \beta \in [0, 1]$ . First, we ensure that  $\gamma_m$  has a minimum value of  $\alpha$ : we do not want to use masked boxes with low confidence because object detection becomes less precise when the mask covers part of the object. Second, we use a higher  $\gamma_m$  if we use a higher  $\gamma_b$  to ensure high precision of ObjectSeeker. To calculate AP for ObjectSeeker, we vary the base confidence threshold  $\gamma_b$  from 0 to 1 with a step of 0.01, change the  $\gamma_m$  correspondingly, and record the precision and recall values

of ObjectSeeker. Then we calculate the averaged precision at different recall values in the conventional way.

We further note that different object detectors (e.g., YOLO vs. Faster RCNN) have different confidence value distributions. For example, the confidence values of most boxes predicted by YOLO could be lower than 0.95 while most Faster RCNN boxes could be more confident than 0.95. As a result, we need to use the clean recall (instead of the confidence threshold) as a universal normalizer when evaluating averaged precision and certified recall. Moreover, we need to adjust  $\alpha, \beta$  for different object detectors and different datasets when deploying the ObjectSeeker defense. In our experiments, we set  $\alpha = 0.8, \beta = 0.8$  for YOLOR on VOC,  $\alpha = 0.7, \beta = 0.5$  for YOLOR on COCO,  $\alpha = 0.8, \beta = 0.5$  for Swin on VOC, and  $\alpha = 0.9, \beta = 0.8$  for Swin on COCO.

**DBSCAN [14] details.** As discussed in Section 3.2, we use DBSCAN to cluster unfiltered masked boxes for box unionizing. DBSCAN is an efficient distance-based clustering algorithm with two parameters  $\epsilon, n$ . It labels a point as a core point when there are at least  $n$  other points whose distances with it are smaller than  $\epsilon$ . All core points and their corresponding neighbors are considered as clusters, and the remaining points are labeled as outliers. In our implementation, we calculate the “distance” between two boxes  $\mathbf{b}_m, \mathbf{b}_b$  as  $1 - \max(\text{IOA}(\mathbf{b}_m, \mathbf{b}_b), \text{IOA}(\mathbf{b}_b, \mathbf{b}_m))$ . We take the maximum because  $\text{IOA}(\cdot, \cdot)$  is an asymmetric operator; we add a negative sign to change the similarity score to distance score. We set  $\epsilon = 0.1, n = 1$  (thus no outliers). We do not report defense performance with different DBSCAN parameters because it only has a minimal effect on the clean performance and no effect on the robustness guarantee.

**Threat models of patch locations.** As discussed in Section 4, we follow DetectorGuard [68] and consider three threat models for patch locations. We consider a patch location as a far-patch when the smallest distance along  $x$  and  $y$  axes between any adversarial pixel and object pixel is larger than 10% of the range of the corresponding axis (i.e., height or width). We consider a patch location as an over-patch when there are adversarial pixels within the bounding box of the object. We consider the remaining patch locations as close-patch.

We will release the source code and omit further discussion of implementation details in the paper.

## B IoU as Similarity Score Function $\mathbb{S}$

In Section 3 and Section 5, we discussed the use of box similar score  $\mathbb{S}$  and noted that different  $\mathbb{S}$  can provide different robustness notions. In this section, we discuss a variant of ObjectSeeker that uses IoU as the similarity score  $\mathbb{S}$  and can certify IoU robustness for the *far-patch threat model*.

The core idea of this ObjectSeeker variant is to split boxes detected on the masked image (masked boxes) into two groups and apply different pruning strategies (with different  $\mathbb{S}$ ) to two groups. The first group contains the boxes that are far

---

**Algorithm 3** ObjectSeeker inference algorithm for IoU robustness

---

**Input:** Image  $\mathbf{x}$ , image size  $(W, H)$ , base object detector  $\mathbb{F}$ , the number lines  $k$  (for masking), masked boxes confidence threshold  $\gamma_m$ , base boxed confidence threshold  $\gamma_b$ , box pruning threshold  $\tau_{\text{IoU}}, \tau_{\text{IoA}}$

**Output:** Robust detection results  $\mathcal{B}_{\text{robust}}$

```

1: procedure DETECTORMASK( $\mathbf{x}, \mathbb{F}, k, W, H, \tau$ )
2:    $\mathcal{M} \leftarrow \text{MASKSET}(k, W, H)$ 
3:    $\mathcal{B}_{\text{mask}}^{\text{no}}, \mathcal{B}_{\text{mask}}^{\text{o}} \leftarrow \emptyset, \emptyset$ 
4:   for  $\mathbf{m} \in \mathcal{M}$  do
5:      $\mathcal{B}_{\mathbf{m}}^{\text{no}}, \mathcal{B}_{\mathbf{m}}^{\text{o}} \leftarrow \text{SPLIT}(\mathbb{F}(\mathbf{x} \odot \mathbf{m}, \gamma_m), \mathbf{m})$ 
6:      $\mathcal{B}_{\text{mask}}^{\text{no}}, \mathcal{B}_{\text{mask}}^{\text{o}} \leftarrow \mathcal{B}_{\text{mask}}^{\text{no}} \cup \mathcal{B}_{\mathbf{m}}^{\text{no}}, \mathcal{B}_{\text{mask}}^{\text{o}} \cup \mathcal{B}_{\mathbf{m}}^{\text{o}}$ 
7:   end for
8:    $\mathcal{B}_{\text{base}} \leftarrow \mathbb{F}(\mathbf{x}, \gamma_b)$ 
9:    $\mathcal{B}_{\text{mask}}^{\text{no-filtered}} \leftarrow \{\mathbf{b}_m \in \mathcal{B}_{\text{mask}}^{\text{no}} \mid \nexists \mathbf{b}_b \in \mathcal{B}_{\text{base}} : \text{IOU}(\mathbf{b}_m, \mathbf{b}_b) > \tau_{\text{IoU}}\}$ 
10:   $\mathcal{B}_{\text{mask}}^{\text{no-pruned}} \leftarrow \text{NMS}(\mathcal{B}_{\text{mask}}^{\text{no-filtered}}, \tau_{\text{IoU}})$ 
11:   $\mathcal{B}_{\text{mask}}^{\text{o-filtered}} \leftarrow \{\mathbf{b}_m \in \mathcal{B}_{\text{mask}}^{\text{o}} \mid \nexists \mathbf{b}_b \in \mathcal{B}_{\text{base}} : \text{IOA}(\mathbf{b}_m, \mathbf{b}_b) > \tau_{\text{IoA}}\}$ 
12:   $\mathcal{B}_{\text{mask}}^{\text{o-pruned}} \leftarrow \{\bigcup_{\hat{\mathbf{b}} \in \hat{\mathcal{B}}} \hat{\mathbf{b}} \mid \hat{\mathcal{B}} \in \text{DBSCAN}(\mathcal{B}_{\text{mask}}^{\text{o-filtered}})\}$ 
13:   $\mathcal{B}_{\text{robust}} \leftarrow \mathcal{B}_{\text{base}} \cup \mathcal{B}_{\text{mask}}^{\text{no-pruned}} \cup \mathcal{B}_{\text{mask}}^{\text{o-pruned}}$ 
14:  return  $\mathcal{B}_{\text{robust}}$ 
15: end procedure

```

---

away from and do not overlap with the masks (termed as *non-overlapping boxes*); the second group considers the boxes that are close to or overlap with the masks (termed as *overlapping boxes*).

When the mask is far away from the given object, the detection of this object is barely affected. As a result, detected non-overlapping masked boxes are almost the same and thus have high pair-wise IoU with each other. We can then easily identify and prune redundant boxes by looking at the IoU. In Lemma 4 and Lemma 5, we can further prove that the IoU-based pruning strategy can provide a certifiable guarantee for IoU certification. After pruning the non-overlapping boxes, we use a similar IoA pruning strategy discussed in the main body to prune overlapping boxes. These boxes can be useful for certifying IoA robustness. We note that we cannot use IoU to prune overlapping boxes because a good number of overlapping boxes only detect part of the object. Therefore, their pair-wise IoU can be too low for an effective pruning.

**Pseudocode.** We present the algorithm pseudocode in Algorithm 3. We first generate the mask set  $\mathcal{M}$  and initialize two empty sets  $\mathcal{B}_{\text{mask}}^{\text{no}}, \mathcal{B}_{\text{mask}}^{\text{o}}$  for holding non-overlapping and overlapping masked boxes (Line 3). Next, we iterate over every mask  $\mathbf{m} \in \mathcal{M}$ . For each mask, we perform object detection on the masked image  $\mathbb{F}(\mathbf{x} \odot \mathbf{m}, \gamma_m)$  and split the detected boxes into non-overlapping boxes  $\mathcal{B}_{\mathbf{m}}^{\text{no}}$  and overlapping boxes  $\mathcal{B}_{\mathbf{m}}^{\text{o}}$  (Line 5). We then add  $\mathcal{B}_{\mathbf{m}}^{\text{no}}$  and  $\mathcal{B}_{\mathbf{m}}^{\text{o}}$  to  $\mathcal{B}_{\text{mask}}^{\text{no}}$  and  $\mathcal{B}_{\text{mask}}^{\text{o}}$ , respectively (Line 6).

After gathering all masked boxes, we further get base boxes  $\mathcal{B}_{\text{base}}$  prediction on the original image (Line 8) and perform secure box pruning on  $\mathcal{B}_{\text{mask}}^{\text{no}}$  (Line 9-10) and  $\mathcal{B}_{\text{mask}}^{\text{o}}$  (Line 11-12) separately. For non-overlapping boxes  $\mathcal{B}_{\text{mask}}^{\text{no}}$ , we first perform box filtering with IoU as the box similarity score  $\mathbb{S}$  (Line 9). Next, we perform non-maximum suppression (NMS) for box clustering and box representing (Line 10). The non-maximum suppression works as follows. First, it picks the box  $\mathbf{b}_0$  with the highest confidence value, finds all boxes  $\mathbf{b}_1$  satisfying  $\text{IoU}(\mathbf{b}_0, \mathbf{b}_1) > \tau_{\text{IoU}}$ , forms a cluster with these boxes. Second, it repeats the first step on remaining unclustered boxes until all boxes are clustered. Third, for each box cluster, it takes the box with highest confidence as the representative. For overlapping boxes  $\mathcal{B}_{\text{mask}}^{\text{o}}$ , we perform box filtering (Line 11) and box unionizing (Line 12) with IoA, similar to what we discussed in Section 3.2.

Finally, we combine base boxes  $\mathcal{B}_{\text{base}}$ , pruned non-overlapping boxes  $\mathcal{B}_{\text{mask}}^{\text{no-pruned}}$  and overlapping boxes  $\mathcal{B}_{\text{mask}}^{\text{o-pruned}}$  together as the final prediction output  $\mathcal{B}_{\text{robust}}$  (Line 13).

**Certification.** The certification with IoU robustness is similar to what we discussed for IoA in Section 3.3. Note that in Line 9 and Line 10 of Algorithm 3, a masked box  $\mathbf{b}_m$  will only be removed when there is another box  $\mathbf{b}_b$  that has a large IoU with  $\mathbf{b}_m$ . Therefore, given a masked box  $\mathbf{b}_m$  and a ground-truth box  $\mathbf{b}_{\text{gt}}$ , we only need to prove the lower bound of  $\text{IoU}(\mathbf{b}_{\text{gt}}, \mathbf{b}_b)$  for any box  $\mathbf{b}_b$  that can remove  $\mathbf{b}_m$  (i.e.,  $\text{IoU}(\mathbf{b}_m, \mathbf{b}_b) > \tau$ ).

**Lemma 4.** *For any ground-truth object box  $\mathbf{b}_{\text{gt}}$ , detected masked box  $\mathbf{b}_m$ , and box  $\mathbf{b}_b$  with  $\text{IoU}(\mathbf{b}_m, \mathbf{b}_b) > \tau$ , we have:*

$$\text{IoU}(\mathbf{b}_{\text{gt}}, \mathbf{b}_b) > \frac{\tau B + (\tau - 1) \cdot C}{A + B + C}, \forall \mathbf{b}_b \text{ s.t. } \text{IoU}(\mathbf{b}_m, \mathbf{b}_b) > \tau$$

where  $A = |\mathbf{b}_{\text{gt}} \setminus \mathbf{b}_m|, B = |\mathbf{b}_{\text{gt}} \cap \mathbf{b}_m|, C = |\mathbf{b}_m \setminus \mathbf{b}_{\text{gt}}|$ .

*Proof.* In this proof, we are going to find the worst-case  $\mathbf{b}_b$  that satisfies the condition of  $\text{IoU}(\mathbf{b}_m, \mathbf{b}_b) > \tau$  but gives the lowest  $\text{IoU}(\mathbf{b}_{\text{gt}}, \mathbf{b}_b)$ .

First, let us divide the box  $\mathbf{b}_b$  into four disjoint parts using set operations.

$$\begin{aligned} \mathbf{b}_b &= (\mathbf{b}_b \cap (\mathbf{b}_{\text{gt}} \cup \mathbf{b}_m)) \cup (\mathbf{b}_b \setminus (\mathbf{b}_{\text{gt}} \cup \mathbf{b}_m)) \\ &= (\mathbf{b}_b \cap (\mathbf{b}_{\text{gt}} \cap \mathbf{b}_m)) \cup (\mathbf{b}_b \cap (\mathbf{b}_m \setminus \mathbf{b}_{\text{gt}})) \cup (\mathbf{b}_b \cap (\mathbf{b}_{\text{gt}} \setminus \mathbf{b}_m)) \\ &\quad \cup (\mathbf{b}_b \setminus (\mathbf{b}_{\text{gt}} \cup \mathbf{b}_m)) \end{aligned}$$

To reason the worst-case  $\text{IoU}(\mathbf{b}_{\text{gt}}, \mathbf{b}_b)$ , we can set the second part  $|\mathbf{b}_b \cap (\mathbf{b}_m \setminus \mathbf{b}_{\text{gt}})|$  to  $|\mathbf{b}_m \setminus \mathbf{b}_{\text{gt}}| = C$  because increasing its area increases  $\text{IoU}(\mathbf{b}_m, \mathbf{b}_b)$  but not  $\text{IoU}(\mathbf{b}_{\text{gt}}, \mathbf{b}_b)$ . We set the third  $|\mathbf{b}_b \cap (\mathbf{b}_{\text{gt}} \setminus \mathbf{b}_m)| = 0$  because decreasing its area decreases  $\text{IoU}(\mathbf{b}_{\text{gt}}, \mathbf{b}_b)$  but not  $\text{IoU}(\mathbf{b}_m, \mathbf{b}_b)$ .

Next, we set the remaining two parts as  $|\mathbf{b}_b \cap (\mathbf{b}_{\text{gt}} \cap \mathbf{b}_m)| = \alpha, |\mathbf{b}_b \setminus (\mathbf{b}_{\text{gt}} \cup \mathbf{b}_m)| = \beta$ . We can then write our constraint sets

as

$$\text{IoU}(\mathbf{b}_m, \mathbf{b}_b) = \frac{|\mathbf{b}_m \cap \mathbf{b}_b|}{|\mathbf{b}_m \cup \mathbf{b}_b|} = \frac{C + \alpha}{B + C + \beta} \geq \tau \quad (1)$$

$$\alpha \geq 0, \beta \geq 0 \quad (2)$$

We can further write the target as:

$$t := \min_{(\alpha, \beta)} \text{IoU}(\mathbf{b}_{\text{gt}}, \mathbf{b}_b) = \frac{\alpha}{A + B + C + \beta} \quad (3)$$

Now it is a linear programming problem for two variables  $\alpha, \beta$ . We can solve it and get the optimal solution as:

$$t^* = \max(0, \frac{\tau B + (\tau - 1) \cdot C}{A + B + C}) := \mathbb{L}_{\text{IoU}}(\mathbf{b}_{\text{gt}}, \mathbf{b}_m, \tau) \quad (4)$$

$$A = |\mathbf{b}_{\text{gt}} \setminus \mathbf{b}_m|, B = |\mathbf{b}_{\text{gt}} \cap \mathbf{b}_m|, C = |\mathbf{b}_m \setminus \mathbf{b}_{\text{gt}}|$$

when  $\beta = 0, \alpha = \max(0, \tau B + (\tau - 1) \cdot C)$ .  $\square$

We use  $\mathbb{L}_{\text{IoU}}(\mathbf{b}_{\text{gt}}, \mathbf{b}_m, \tau)$  to denote this new bound for IoU. Next, we present the following lemma to demonstrate that  $\mathbb{L}_{\text{IoU}} > T$  is the sufficient condition of being a pruning-safe masked box.

**Lemma 5.** *Given a ground-truth object  $\mathbf{b}_{\text{gt}}$  and the IoU pruning threshold  $\tau$ , if there is one masked box  $\mathbf{b}_m \in \mathcal{B}_{\text{mask}}^{\text{no}}$  satisfying that  $\mathbb{L}_{\text{IoU}}(\mathbf{b}_{\text{gt}}, \mathbf{b}_m, \tau) > T$ , this box is a pruning-safe masked box for object  $\mathbf{b}_{\text{gt}}$  in IOU-BOXPRUNE, i.e.,  $\exists \mathbf{b}' \in \mathcal{B}_{\text{robust}}$  s.t.  $\text{IoU}(\mathbf{b}_{\text{gt}}, \mathbf{b}') > T$ .*

*Proof.* The detected masked box  $\mathbf{b}_m \in \mathcal{B}_{\text{mask}}^{\text{no}}$  will go through box filtering (Line 9 of Algorithm 3) and box unionizing (Line 10 of Algorithm 3) to generate the final output. We will demonstrate this masked box  $\mathbf{b}_m$  will “survive” these two operations and become part of the final output, ensuring the IoU robustness. There are three possible cases for the masked box  $\mathbf{b}_m$  going through the box filtering and the box unionizing processes.

1.  $\mathbf{b}_m$  is filtered in the box filtering process (Line 9). Then there is a base box  $\mathbf{b}_b \in \mathcal{B}_{\text{base}}$  satisfying  $\text{IoU}(\mathbf{b}_m, \mathbf{b}_b) > \tau$ . From Lemma 4, we know there is a box  $\mathbf{b}' = \mathbf{b}_b \in \mathcal{B}_{\text{base}} \subset \mathcal{B}_{\text{robust}}$  satisfies  $\text{IoU}(\mathbf{b}_{\text{gt}}, \mathbf{b}') > \mathbb{L}_{\text{IoU}}(\mathbf{b}_{\text{gt}}, \mathbf{b}_m, \tau) > T$ .
2.  $\mathbf{b}_m$  is removed in the box unionizing step (Line 10). This implies that there is another masked box  $\mathbf{b}'_m \in \mathcal{B}_{\text{mask}}^{\text{no-filtered}}$  satisfying  $\text{IoU}(\mathbf{b}_m, \mathbf{b}'_m) > \tau$ . From Lemma 4, we know there is a box  $\mathbf{b}' = \mathbf{b}'_m \in \mathcal{B}_{\text{mask}}^{\text{no-pruned}} \subset \mathcal{B}_{\text{robust}}$  satisfies  $\text{IoU}(\mathbf{b}_{\text{gt}}, \mathbf{b}') > \mathbb{L}_{\text{IoU}}(\mathbf{b}_{\text{gt}}, \mathbf{b}_m, \tau) > T$ .
3.  $\mathbf{b}_m$  is not removed and becomes a part of  $\mathcal{B}_{\text{mask}}^{\text{no-pruned}} \subset \mathcal{B}_{\text{robust}}$ . Then we know there is a box  $\mathbf{b}' = \mathbf{b}_m \in \mathcal{B}_{\text{robust}}$  such that  $\text{IoU}(\mathbf{b}_{\text{gt}}, \mathbf{b}') = |\mathbf{b}_{\text{gt}} \cap \mathbf{b}_m| / |\mathbf{b}_{\text{gt}} \cup \mathbf{b}_m| \geq \mathbb{L}_{\text{IoA}}(\mathbf{b}_{\text{gt}}, \mathbf{b}_m, \tau) > T$ .

$\square$

Table 4: Defense performance of ObjectSeeker with IoU robustness (Algorithm 3)

Dataset		PASCAL VOC		MS COCO		
Defense	Metric	Certify class?	AP <sub>50</sub>	IoU-CertR@0.8 ( $T = 0.5$ ) far-patch	AP <sub>50</sub>	IoU-CertR@0.6 ( $T = 0.5$ ) far-patch
ObjectSeeker-YOLOR		✓	92.8%	48.3%	69.2%	37.8%
ObjectSeeker-Swin			92.0%	34.9%	68.6%	28.6%

With Lemma 4 and Lemma 5, the certification is straightforward: we only need to replace the certification condition with the new bound  $\mathbb{L}_{\text{IoU}}(\mathbf{b}_{\text{gt}}, \mathbf{b}_{\text{m}}, \tau) > T$  in Line 6 of Algorithm 2.

**Implementation and performance evaluation.** In our implementation, we consider a box is a non-overlapping box if the smallest distance between the masked box and the mask along  $x$  and  $y$  axes is larger than 5% of the range of the corresponding axis (i.e., height or width). We use the same setup as in Section 4 to evaluate Algorithm 3. We set  $\tau_{\text{IoU}} = 0.8$  and the IoU certification threshold  $T_{\text{IoU}} = 0.5$  and report the defense performance in Table 4. As shown in the table, Algorithm 3 has similarly high clean AP as Algorithm 1 (recall Table 2), and more importantly, achieves the first certified IoU robustness against patch hiding attacks.

## C Taxonomy of Robustness Notions against Hiding Attacks

In the main body of this paper, we focus on IoA robustness; in Appendix B, we further presented a ObjectSeeker variant that has IoU robustness against far-patch attackers. In this section, we aim to provide a taxonomy of different robustness notions against hiding attacks to shed a light on future research. We summarize four major robustness notions in Table 5, which are categorized based on two important robustness factors as discussed next.

**Factor 1: attack detection vs. robust prediction.** The first factor to consider in robustness notions is the defense format: attack detection versus robust prediction. An attack-detection defense aims to detect an attack: it alerts and abstains from making predictions when it detects an attack. Formally, we allow the defense to output a special symbol  $\perp$  for cases when it detects an attack. Then, a defender aims to build a robust object detector  $\mathbb{F}$  that minimizes the following quantity of “adversarial risk”.

$$\min_{\mathbb{F}} \left( \mathbb{E}_{\mathbf{x}, \mathbf{b}_{\text{gt}}} \left[ \max_{\mathbf{x}' \in \mathcal{A}_p(\mathbf{x}); \mathbb{F}(\mathbf{x}') \neq \perp} \ell(\mathbf{b}_{\text{gt}}, \mathbb{F}(\mathbf{x}')) \right] \right)$$

where  $\mathbf{b}_{\text{gt}}$  is a ground-truth box/object on the image  $\mathbf{x}$  (here we consider one object for simplicity),  $\mathbf{x}'$  is an adversarial image (within the threat model), and  $\ell$  is a loss function for measuring and correctness/quality of the predicted box (the loss function is determined by the requirement of box quality that will be discussed in Factor 2). The inner max operation

Table 5: Taxonomy of robustness notions against hiding attacks

	Attack detection	Robust prediction
IoA robustness	<b>Notion I</b> DetectorGuard [68]	<b>Notion II</b> ObjectSeeker (Section 3)
IoU robustness	<b>Notion III</b> –	<b>Notion IV</b> ObjectSeeker (Appendix B)

corresponds to the definition of adversarial risk: an attacker aims to maximize the loss for the output box  $\ell(\mathbf{b}_{\text{gt}}, \mathbb{F}(\mathbf{x}'))$  while *not triggering an attack alert* ( $\mathbb{F}(\mathbf{x}') \neq \perp$ ).

In contrast, a robust-prediction defense does not involve the abstention symbol  $\perp$ ; its objective is to minimize the following “adversarial risk”.

$$\min_{\mathbb{F}} \left( \mathbb{E}_{\mathbf{x}, \mathbf{b}_{\text{gt}}} \left[ \max_{\mathbf{x}' \in \mathcal{A}_p(\mathbf{x})} \ell(\mathbf{b}_{\text{gt}}, \mathbb{F}(\mathbf{x}')) \right] \right)$$

We can see that this new definition relaxes the condition of  $\mathbb{F}(\mathbf{x}') \neq \perp$  (not alerting), making the attack easier and the defense harder. Therefore, the robust-prediction defense provides a stronger robustness notion.

We note that in addition to the theoretical strengths as discussed above, robust-prediction defenses also have advantages in practice. First, robust-prediction defenses have the guarantee for availability since the defense never abstains from making predictions, in contrast to attack-detection defenses’ vulnerability to Denial-of-Service attacks. Second, in the clean setting, robust-prediction defenses do not have false alerts that can be confusing and downgrade the user experience.

Finally, we note that DetectorGuard [68] is an attack-detection defense (Notion I) while ObjectSeeker aims to build a robust-prediction defense (Notion II and IV).

**Factor 2: IoA robustness vs. IoU robustness.** The second factor is about the guarantee for the box quality: IoA robustness versus IoU robustness. In the main body of this paper, we consider IoA robustness because it aligns with the defense objective against patch hiding attacks: we aim to detect at least part of the object ( $\text{IoA}(\mathbf{b}_{\text{gt}}, \mathbf{b}') = |\mathbf{b}_{\text{gt}} \cap \mathbf{b}'| / |\mathbf{b}_{\text{gt}}| > T$ ).<sup>8</sup>

However, a defense with IoA robustness might end up predicting large bounding boxes that cover the entire image.

<sup>8</sup>One possible loss  $\ell$  for this objective can be  $\ell(\mathbf{b}_{\text{gt}}, \mathbf{b}') = \max(0, T - \text{IoA}(\mathbf{b}_{\text{gt}}, \mathbf{b}'))$ .

When this happens, the IoA robustness is satisfied (IoA equals to 1), but the defense output is not ideal: we only know that there are objects of certain classes but do not know the object locations. Therefore, we are motivated to consider the concept of IoU robustness ( $\text{IoU}(\mathbf{b}_{\text{gt}}, \mathbf{b}') = |\mathbf{b}_{\text{gt}} \cap \mathbf{b}'| / |\mathbf{b}_{\text{gt}} \cup \mathbf{b}'| > T$ ), which adds additional constraints on the sizes of predicted boxes. In Appendix B, we discuss a variant of ObjectSeeker that can certify IoU robustness against far-patch attackers.

**Remark: the connection between Notion II and Notion I.** As shown in Table 5, both Notion I and Notion II use IoA robustness, and they differ in the defense formats of attack detection versus robust prediction. Here, we can demonstrate the equivalence of two notions in terms of certified robustness, which further uncovers the subtle issue of the IoA robustness and motivates the notion of IoU robustness.

First, we can build a Notion I defense with a Notion II defense. This is directly implied by the definition: any Notion II defense is a valid Notion I defense that relinquishes the freedom of issuing alerts.

Second, counterintuitively, we can also build a Notion II defense with a Notion I defense. The strategy is, if the Notion I defense detects an attack, instead of issuing an alert, it outputs large bounding boxes of all different classes to cover the entire image. Since these large boxes have IoAs of 1 for any object of the same object class, the defense is considered as IoA-robust.<sup>9</sup>

*Note 1: empirical advantage of Notion II defenses.* Despite the equivalence in certifiable robustness with Notion I defenses, Notion II defenses still have advantages in terms of empirical performance. For example, when there is a false alert in the clean setting, a Notion I based defense would either alert or output useless large boxes while a Notion II defense can still predict reasonable boxes (e.g. boxes that obtain high IoU with the ground-truth objects).

*Note 2: the necessity of box unionizing in ObjectSeeker.* Given the reduction strategies between Notion I and Notion II defenses, one might question the necessity and value of the box unionizing module in our ObjectSeeker design (since it can be replaced with an attack alert module or a large box outputting module with no cost of certifiable robustness). Here, we want to reiterate that ObjectSeeker is defense framework and is compatible with different box similarity score functions  $\mathbb{S}$  such as IoA and IoU, while the reduction problem discussed above is only for the IoA robustness. When we use IoU as the score function  $\mathbb{S}$  and consider IoU robustness, the box unionizing is necessary since we can no longer output large boxes discussed for IoA. Another benefit of having box unionizing is the empirical advantage discussed in the paragraph above.

**Factor 3: Protect class labels or not.** In addition to two robustness factors presented in Table 5, we can further categorize robustness notions based on whether the defense protects

<sup>9</sup>We note that an extremely large box has a small IoU with the ground-truth box; therefore, this strategy of outputting large boxes does not apply to Notion III and Notion IV where we consider IoU robustness.

the class label or not. For example, DetectorGuard [68] is fundamentally limited in its design not to be able to certify class labels. In contrast, ObjectSeeker is flexible for the class label certification. We note that this is another advantage of ObjectSeeker over DetectorGuard.

**Future of robust object detection.** As a summary of this section, we believe that the ultimate goal of certifiably robust defenses against patch hiding attacks is a robust-prediction defense with IoU robustness (Notion IV). The defense problem can then be interpreted as a list decoding problem: we aim to output a list of bounding boxes such that a subset of bounding boxes have high IoUs with all ground-truth boxes. Furthermore, we can also consider a stronger attacker who also wants to increase FP errors. We can deploy an empirical defense via classifying all predicted bounding boxes and removing boxes with inconsistent labels [68].

## D ObjectSeeker against Multiple Patches

In this paper, we focus on certifiably robust defenses against *one-patch* hiding attacks, and we design a patch-agnostic masking technique (Section 3.1) for this task. The strategy for patch-agnostic masking against multiple patches is an open research question; in this section, we provide a proof-of-concept for defending against two patches using the prior knowledge of patch shapes and sizes. We note that the design of ObjectSeeker is general: we can plug a different mask set  $\mathcal{M}$  into Algorithm 1 for defending against different patch attackers as long as some masks can remove all adversarial pixels.

To generate a set of masks that simultaneously mask out two regions (patches) of the input image, we adopt the mask set generation technique from PatchCleanser [67], state-of-the-art certifiably robust image classification defense against adversarial patches. The high-level idea is to move large masks over the input images while using a larger stride to skip a number of mask locations to improve efficiency. The mask shape, size, and stride are carefully determined so that at least some masks can remove the entire patch [67].

In our experiment, we consider two square 0.5%-pixel patches. We first generate a mask set  $\mathcal{M}'$  that has 100 masks, at least one of which can remove one 0.5%-pixel patch regardless of the patch location. We then generate another mask set  $\mathcal{M}$  that contains all possible two-mask combinations from the mask set  $\mathcal{M}'$  to instantiate ObjectSeeker. We note that the number masks in this experiment is extremely large (5k); therefore, we only evaluate the defense with YOLOR on 50 test images of the VOC dataset. Furthermore, since the number of two patch locations can also be too large to evaluate, we only uniformly select 1/50 of all possible patch locations for robustness certification.

We report the defense performance in Table 7. First, we can see that our defense still has high clean performance. Second, ObjectSeeker achieves high robustness against far-

Table 6: Performance of vanilla undefended models, ObjectSeeker, and DetectorGuard [68] on KITTI [17]

Model \ Metric	Certify class?	YOLOR [62]					Swin [35]				
		AP <sub>0.5</sub>	FAR	Certified recall (@0.8)			AP <sub>0.5</sub>	FAR	Certified recall (@0.8)		
				far-patch	close-patch	over-patch			far-patch	close-patch	over-patch
Vanilla (undefended)	–	93.2%	–	–	–	–	89.5%	–	–	–	–
ObjectSeeker	✓	92.9%	–	82.3%	48.9%	10.3%	89.4%	–	68.8%	43.7%	10.5%
ObjectSeeker	✗	93.0%	–	82.6%	49.0%	10.3%	89.4%	–	69.0%	43.8%	10.6%
DetectorGuard [68]	✗	93.0%	0.2%	24.2%	8.3%	0.7%	89.4%	0.1%	23.9%	8.3%	0.7%

Table 7: Defense performance against two 0.5%-pixel square patches for 50 VOC test images

Model \ Metric	AP <sub>0.5</sub>	Certified recall (@0.8)		
		far-patch	close-patch	over-patch
YOLOR	98.0%	–	–	–
ObjectSeeker-YOLOR	98.0%	51.6%	21.3%	3.3%

patch; in contrast, the certified recall for close-patch and over-patch is greatly reduced from the results reported in Table 2 (for one 1%-pixel patch). These observations align with the DetectorGuard paper [68]: multiple patches have to be close to each others to have greater malicious effects. How to further improve the defense performance for close-patch and over-patch is one of our future work directions.

## E Additional Experiment Results

In this section, we report additional experiment results for different datasets to further demonstrate the general applicability of ObjectSeeker. We first report defense performance for an additional dataset KITTI [17], we then include detailed analysis for YOLOR and COCO (similar to what we have in Section 4.3 for YOLOR and VOC).

**Additional evaluation for KITTI [17].** KITTI is a dataset for autonomous driving applications, which contains both 2D camera images and 3D point clouds. Following DetectorGuard [68]. We use 80% of its 7481 2D images for training and the remaining 20% for validation. We merge all classes into three classes: *car* (all different classes of vehicles), *pedestrian*, *cyclist*. We use the same set of defense parameters of VOC to instantiate ObjectSeeker for KITTI. We then report the defense performance of ObjectSeeker and DetectorGuard [68] in Table 6. As shown in the table, ObjectSeeker has a similarly high clean performance as vanilla undefended models and achieves significantly higher certified recall than DetectorGuard [68]; the observation is similar to that of Table 2 in Section 4.2. We note that the CertR@0.8 of ObjectSeeker-YOLOR for far-patch becomes larger than 80% (the clean recall value); this is possible because we are setting the certification threshold  $T = 0$ , which is an easier condition to satisfy compared to the condition for clean evaluation (requiring IoU is larger than 0.5).

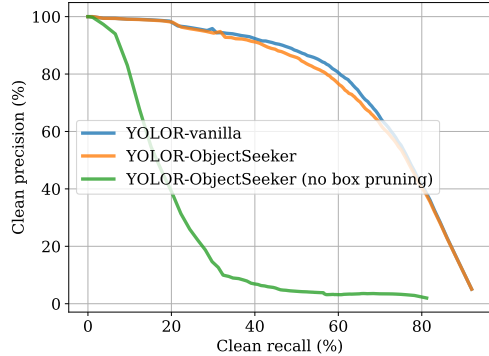


Figure 11: Clean precision vs. clean recall (COCO)

**Additional experiment results for COCO.** In Figure 11 and Figure 12, we plot the clean precision-recall curve and the CertR-recall curve for COCO. The observation is similar to that for VOC in Section 4.3. We note that the certified recall of COCO does not further increase as clean recall exceeds 70%. This is because, the masked box confidence threshold  $\gamma_m = \max(\alpha, \gamma_b + (1 - \gamma_b) \cdot \beta)$  starts to take the value  $\alpha$  when  $\gamma_b$  takes a low value.

In Figure 13, Figure 14, and Figure 15, we report defense performance with different defense parameters  $k, \gamma_m, \tau$ . In Figure 16 and Figure 17, we further report certified robustness with a larger certification threshold  $T$  and against a larger patch. The observations from these figures are similar to those reported for VOC in Section 4.3. This further demonstrates that ObjectSeeker works well for both easier and harder object detection tasks.

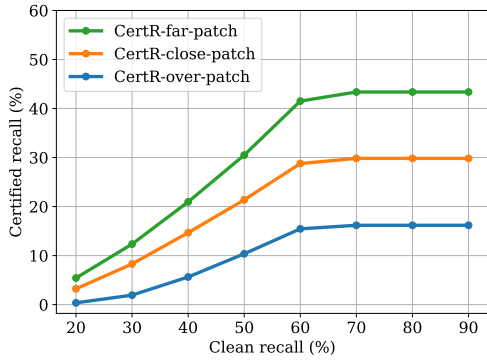


Figure 12: Certified recall vs. clean recall (COCO)

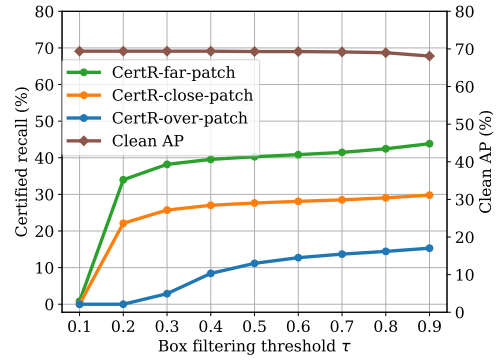


Figure 15: Effect of box filtering threshold  $\tau$  (COCO)

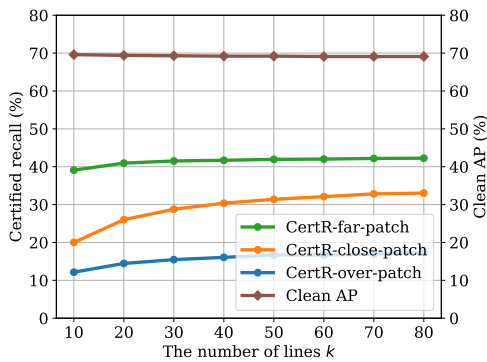


Figure 13: Effect of the number of lines  $k$  (COCO)

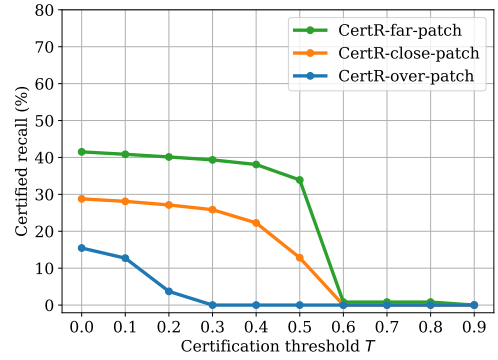


Figure 16: ObjectSeeker performance for different certification thresholds  $T$  (COCO)

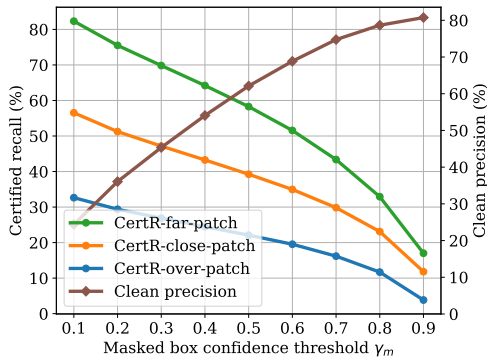


Figure 14: Effect of masked box confidence threshold  $\gamma_m$  (COCO)

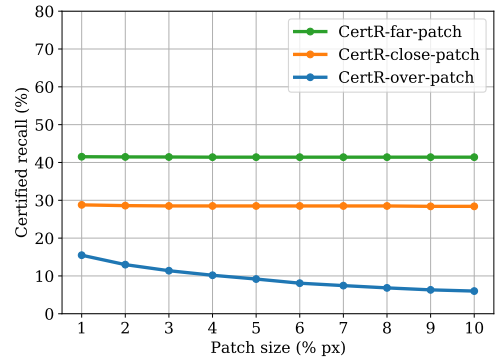


Figure 17: ObjectSeeker performance against different patch sizes (COCO)